
# NAVAL POSTGRADUATE SCHOOL

**MONTEREY, CALIFORNIA**

# THESIS

**SURVIVABILITY ENHANCEMENT IN A COMBAT ENVIRONMENT**

by

Seow, Yoke Wei

December 2004

| | |
|---|---|
| Thesis Advisor: | Daphne Kapolka |
| Second Reader: | Robert Hutchins |

**THIS PAGE INTENTIONALLY LEFT BLANK**

| REPORT DOCUMENTATION PAGE | | | Form Approved OMB No. 0704-0188 |
|---|---|---|---|
| Public reporting burden for this collection of information is estimated to average 1 hour per response, including the time for reviewing instruction, searching existing data sources, gathering and maintaining the data needed, and completing and reviewing the collection of information. Send comments regarding this burden estimate or any other aspect of this collection of information, including suggestions for reducing this burden, to Washington headquarters Services, Directorate for Information Operations and Reports, 1215 Jefferson Davis Highway, Suite 1204, Arlington, VA 22202-4302, and to the Office of Management and Budget, Paperwork Reduction Project (0704-0188) Washington DC 20503. | | | |
| **1. AGENCY USE ONLY** ***(Leave blank)*** | **2. REPORT DATE** December 2004 | **3. REPORT TYPE AND DATES COVERED** Master's Thesis | |
| **4. TITLE AND SUBTITLE**: Title (Mix case letters) Survivability Enhancement in a Combat Environment | | | **5. FUNDING NUMBERS** |
| **6. AUTHOR(S)** Mr Seow Yoke Wei, The Republic of Singapore | | | |
| **7. PERFORMING ORGANIZATION NAME(S) AND ADDRESS(ES)** Naval Postgraduate School Monterey, CA 93943-5000 | | | **8. PERFORMING ORGANIZATION REPORT NUMBER** |
| **9. SPONSORING /MONITORING AGENCY NAME(S) AND ADDRESS(ES)** N/A | | | **10. SPONSORING/MONITORING AGENCY REPORT NUMBER** |
| **11. SUPPLEMENTARY NOTES** The views expressed in this thesis are those of the author and do not reflect the official policy or position of the Department of Defense or the U.S. Government. | | | |
| **12a. DISTRIBUTION / AVAILABILITY STATEMENT** Approved for public release; distribution is unlimited. | | | **12b. DISTRIBUTION CODE** A |


**13. ABSTRACT (maximum 200 words)**

The objective of this thesis is to provide an aircraft with an optimal route to its destination that avoids encroaching into surface-to-air weapons killing envelopes in real time. The optimal route computed will be updated dynamically, depending on the location of the vehicle and the location of the Surface to Air Missile (SAM) sites. The problem was solved using heuristic algorithms instead of the conventional *Dijkstra's & Bellman Ford* algorithms, which are computationally expensive. Data fusion techniques such as spatial correlation and triangulation algorithms are presented in detail. Such techniques are important for situational awareness in a real time combat environment. Important information provided by onboard sensors are merged with the preplanned data to provide the operator with a better integrated picture of the combat environment.


| **14. SUBJECT TERMS** Kill envelopes of surface-to-air missile sites, circular error probable (CEP), uncertainty ellipse, correlation, bearings triangulation, optimal route, route planning, data fusion. | | | **15. NUMBER OF PAGES** 77 |
|---|---|---|---|
| | | | **16. PRICE CODE** |
| **17. SECURITY CLASSIFICATION OF REPORT** Unclassified | **18. SECURITY CLASSIFICATION OF THIS PAGE** Unclassified | **19. SECURITY CLASSIFICATION OF ABSTRACT** Unclassified | **20. LIMITATION OF ABSTRACT** UL |

NSN 7540-01-280-5500 Standard Form 298 (Rev. 2-89)
Prescribed by ANSI Std. 239-18

**THIS PAGE INTENTIONALLY LEFT BLANK**

**Approved for public release; distribution is unlimited**

**SURVIVABILITY ENHANCEMENT IN A COMBAT ENVIRONMENT**

Seow, Yoke Wei
Civilian, Singapore Ministry of Defense
B. S., National University of Singapore, 1996

Submitted in partial fulfillment of the
requirements for the degree of

**MASTER OF SCIENCE IN COMBAT SYSTEMS TECHNOLOGY**

from the

**NAVAL POSTGRADUATE SCHOOL**
**December 2004**

Author: Seow, Yoke Wei

Approved by: Daphne Kapolka
Thesis Advisor

Robert Hutchins
Second Reader

James H. Luscombe
Chairman, Department of Physics

**THIS PAGE INTENTIONALLY LEFT BLANK**

# ABSTRACT

The objective of this thesis is to provide an aircraft with an optimal route to its destination that avoids encroaching into surface-to-air weapons killing envelopes in real time. The optimal route computed will be updated dynamically, depending on the location of the vehicle and the location of the Surface to Air Missile (SAM) sites. The problem was solved using heuristic algorithms instead of the conventional Dijkstra and Bellman Ford algorithms, which are computationally expensive. Data fusion techniques such as bearings triangulation, spatial correlation and ellipses combination algorithms are presented in detail. Such techniques are important for situational awareness in a real time combat environment. Important information provided by onboard sensors are merged with the preplanned data to provide the operator with a better-integrated picture of the combat environment.

**THIS PAGE INTENTIONALLY LEFT BLANK**

## TABLE OF CONTENTS

**THIS PAGE INTENTIONALLY LEFT BLANK**

# LIST OF FIGURES

# ACKNOWLEDGMENTS

The author would like to express his gratitude towards Professors Daphne Kapolka and Robert Hutchins for their guidance, advice, encouragement and patience in helping him complete this thesis.

Lastly, the author would like to take this opportunity to acknowledge the tremendous support given by his lovely wife, Carol and wonderful daughter, Amandel. Without their companionship and encouragement, the completion of this thesis would not have been possible.

**THIS PAGE INTENTIONALLY LEFT BLANK**

# I. INTRODUCTION

The ability to exploit crucial threat information *accurately*, *rapidly* and *safely* can greatly enhance the survivability of an airborne vehicle such as an Unmanned Aerial Vehicle *(UAV)* or piloted fixed wing aircraft, especially when engaged in a combat environment. Achieving good situational awareness of the combat environment at standoff ranges has produced major advances in target detection/tracking, surveillance/reconnaissance and battlefield awareness for many applications, including precision strike, command and control, and air and missile defense.

This thesis addresses two fundamental aspects of the control and navigation problem for aircraft operating in hostile territory. The first of which is to obtain an optimal route to and from the target that avoids enemy fire when the positions of such weapons are changing. The second is to locate the enemies' radar sites to within a desired circular error probable (CEP) using spatial correlation technique. The concept presented represents a substantial improvement in aircraft navigation and target location.

## A. OBJECTIVE OF THE OPTIMAL ROUTE

The objective of the optimal route developed in this thesis is to provide a fixed wing aircraft, either manned or unmanned, a route from the platform's current location to its preplanned destination. The computed optimal route will avoid encroaching into all known enemy's SAM (Surface to Air Missile) sites. The data on site locations may be obtained prior to flight (and hence be preplanned), or updated during flight via data link or located during flight by on board sensors. The requirements and constraints imposed in the construction of the optimal route addressed in this thesis are not suitable for helicopters because of their greater maneuverability.

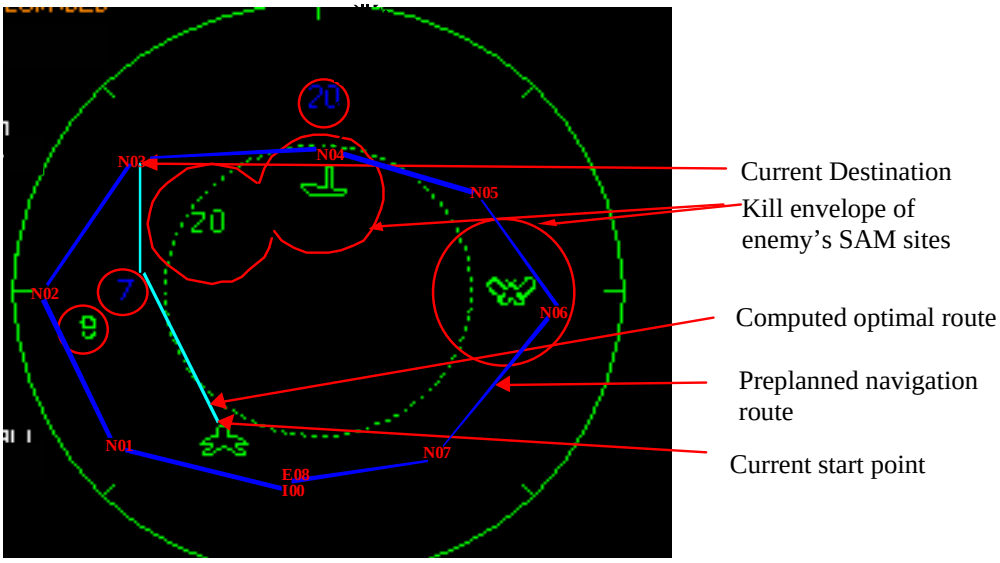


Figure 1. Example of an aircraft monitor showing an optimal route in the combat environment.

A typical optimal route appears as shown in Figure 1 for a set of known kill envelope locations, in which the radius of the kill envelope represents the effective range of the surface to air missile.

. The active leg, i.e. the one the aircraft is steering toward, is presented with a solid line while the non-active legs are presented with dotted lines.

In this thesis, we consider a *two-dimensional* flight plan of an aircraft. We are interested in finding the optimal route of a single aircraft engaged in a surveillance/reconnaissance mission. The problem will be addressed as a large-scale dynamic programming problem [5].

## B. ALGORITHMS AND METHODOLOGY

Similar problems have been solved using the conventional Dijkstra's & Bellman Ford algorithms. These algorithms function by constructing a shortest-path tree from the initial vertex to every other vertex. Constructing a shortest-path tree is computationally expensive, especially when the number of vertices involved in the problem is large. These algorithms are usually used in computer networking but not to solve real time problems. In this thesis, heuristic algorithms, which are computationally efficient, are used to solve the problem. By employing the divide and conquer methodology, the problem is broken down into three sub categories, namely:

- Geometric construction.
- Approximate route construction.
- Route dynamic programming

The details of each of the above will be discussed in Chapter II.

## C. PERFORMANCE AND OUTPUT

The complexity of the computation depends on the distance between the start and destination pair, the number and locations of the SAM sites kill envelopes and the rate of information update by the sensors. The proposed dynamic and robust heuristic algorithms provide a real time solution to the problem with a typical run time of about 200ms for a scenario consisting of sixteen SAM sites using a Pentium 3 CPU.

The error of the computed route should not exceed 8% from the 'true' route. The usual acceptable error figure is about 10% (a ballpark figure provided by test engineers). The 8% quoted is a figure achieved by comparing the length of the optimal route computed using the heuristic algorithms with those computed manually (by brute force) on a case by case basis.

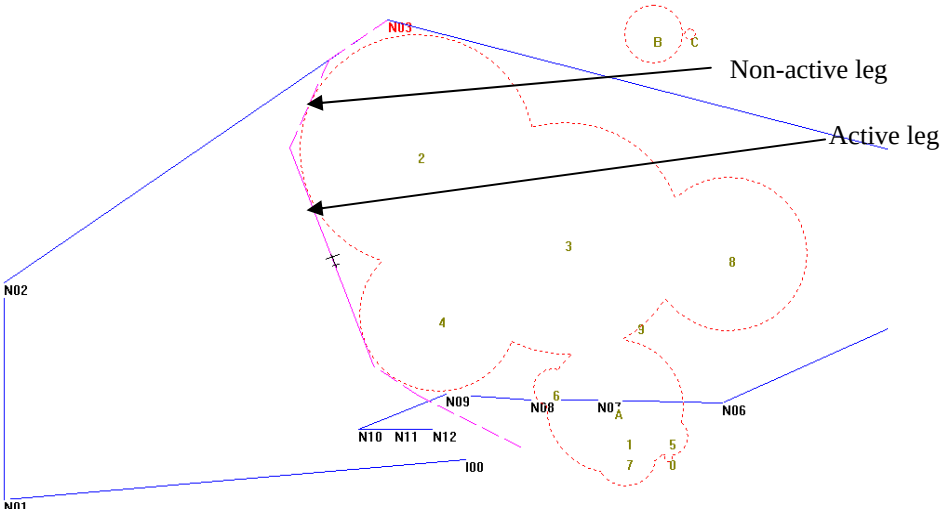


Figure 2. A typical optimal route.

Figure 2 shows the dynamic update of the route when the location of the kill envelope of SAM site number 3 is updated by on board sensors. The new location of SAM site 3 rendered the current optimal route invalid; hence a new route is recomputed.

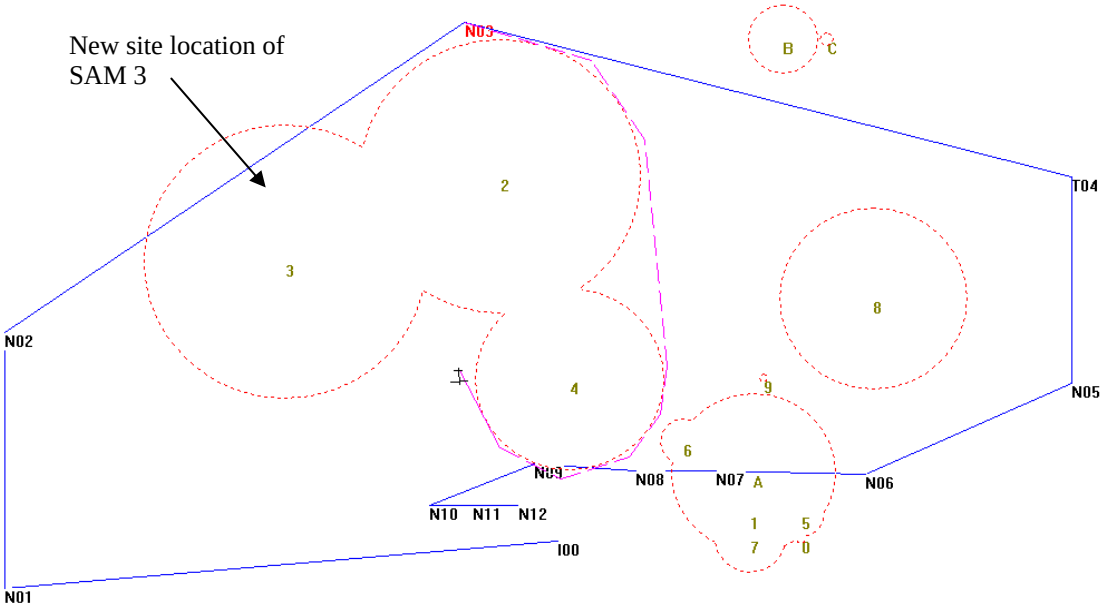


Figure 3. An optimal route which avoids encroaching into all kill envelopes is recomputed because the new site formed (site 3) intersects the previously computed route.

## D. OBJECTIVE OF THE SPATIAL CORRELATION

When an emitter is detected in its search mode, it is usually not threatening [3]. But if it is switched from search to lock-on (i.e. the radar is tracking the platform), then the operator's attention must be drawn to it immediately. In a combat environment, radars can change their operating parameters and frequencies in order to make their detection and location difficult. Hence it is important that the real time information collected by onboard sensors, such as ELS (Emitter Locator Sensor) be improved by data fusion techniques to minimize the time required to locate the enemy radar to a desirable CEP[1] (Circular Error Probable).

The objective of spatial correlation is to optimize the use of real time ELS bearing information to minimize the CEP improvement time. The term active ellipse is used to refer to an ellipse whose CEP and location are currently being updated by the ELS. This is achieved by correlating the active ellipse or CEP, computed by the ELS to the preplanned ellipse representing the SAM site to achieve a resultant ellipse whose CEP is significantly smaller than that computed by the ELS alone. The time reduction to achieve the desirable CEP depends on the orientation of the ellipses, which in turn depends on the flight profile. The resultant CEP is always better than the ellipse computed by the ELS alone.

## E. ALGORITHMS AND LOGIC

The position of a stationary radiating emitter can be estimated from the measurement of the relative direction of arrival of electromagnetic waves received at various locations [6]. Figure 4 shows the triangulation of all the bearing lines collected by the aircraft in the absence of noise or errors. All bearing lines intersect at the same point.

[1] CEP gives the range within which there is a specified probability of finding an object. For instance, a CEP of 10 meters with a 50% probability means that there is a 50% probability of finding the object to within a radius of 10 meters from the center of the circle.

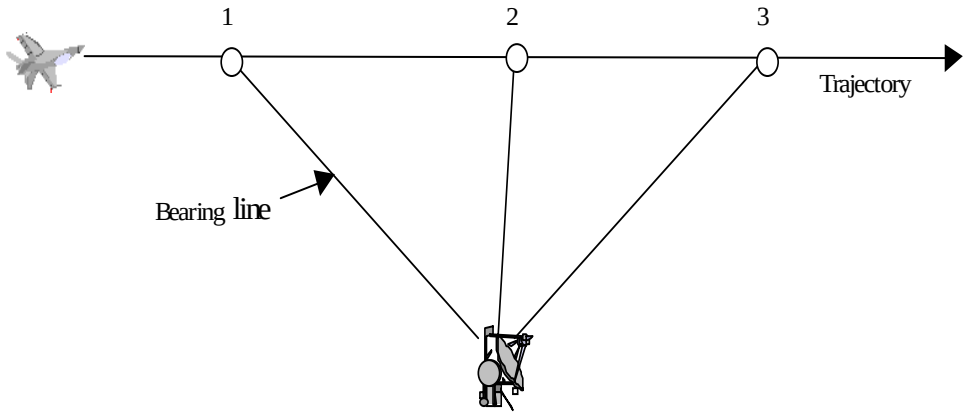


Figure 4. The triangulation of bearing lines arriving from a stationary ground emitter without error.

With noise or errors, the triangulation of the bearing lines forms an ellipse. The size of the ellipse can be quantified by a CEP, which represents the uncertainty in the location of the ground emitter. The details of this calculation are provided in Chapter III.

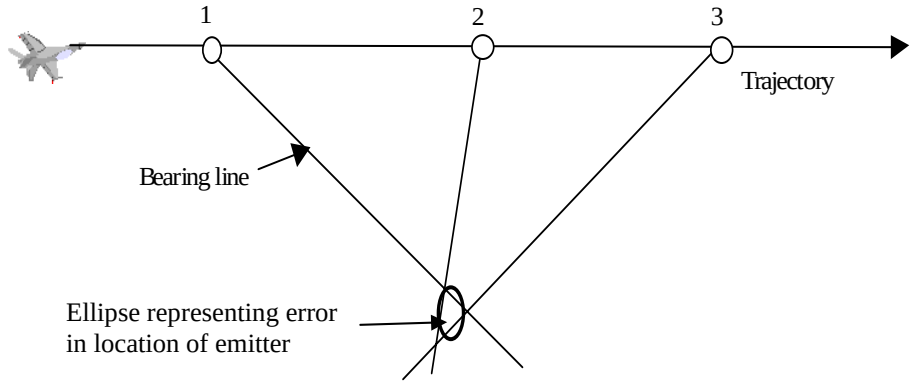


Figure 5. The triangulation of bearing lines arriving from a stationary ground emitter with errors.

Consider the following scenario: An ellipse representing a preplanned SAM site, with a certain predefined CEP value and orientation was uploaded into the database of the mission computer of the navigation vehicle. The onboard sensor detects a signal, which corresponds to the same weapon system. The triangulation of the active bearing lines gives the signal location represented by an ellipse, which is spatially close to that of the preplanned site. The two ellipses can be correlated and combined to form a third ellipse, whose location is better than the parent ellipses. Figure 6 shows the result of the correlation and combination of the ellipses.

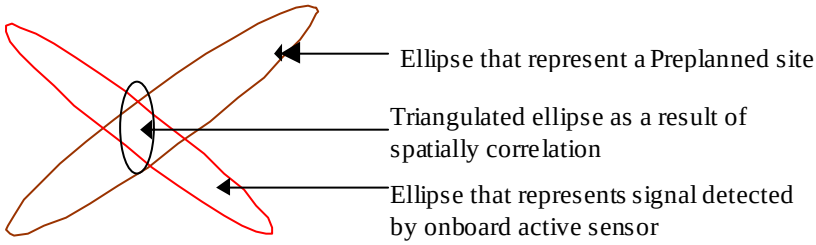


Figure 6. The correlation of an active signal with preplanned site. Combination of the two ellipses to form a third ellipse.

## F. OUTPUT AND OPERATIONAL REQUIREMENTS

The ellipse information is presented using the following parameters:

a. Center of ellipse in Cartesian coordinates

b. Length of major axis and minor axis of ellipse

c. Orientation of ellipse with respect to x-axis. This is defined by the angle subtended by the major axis with the x-axis, measured in the clockwise direction.

In order to achieve the best CEP in the shortest amount of time, the preplanned ellipse must be oriented at ninety degree with respect to the ellipse computed by the ELS. When this happens, the two ellipses ‘cut’ optimally and produce the smallest resultant ellipse.

**THIS PAGE INTENTIONALLY LEFT BLANK**

# II. CONSTRUCTION OF THE OPTIMAL ROUTE

This chapter addresses the algorithms and technical details used to construct the optimal route. They are subdivided into three sections, namely geometric construction, approximate route construction and route dynamic programming. The dynamic behavior of the optimal route will be illustrated with examples and some interesting scenarios will be presented at the end of the chapter.

## A. GEOMETRIC REPRESENTATION OF THE SURFACE-TO-AIR WEAPON KILL ENVELOPES

In a two-dimensional display, the surface-to-air weapon kill envelopes can be represented by circles, whose radii represent the surface-to-air missile kill ranges. In three-dimensional display, these kill envelopes are represented by dome shape encolsure. Therefore, their radii vary according to altitude [1].

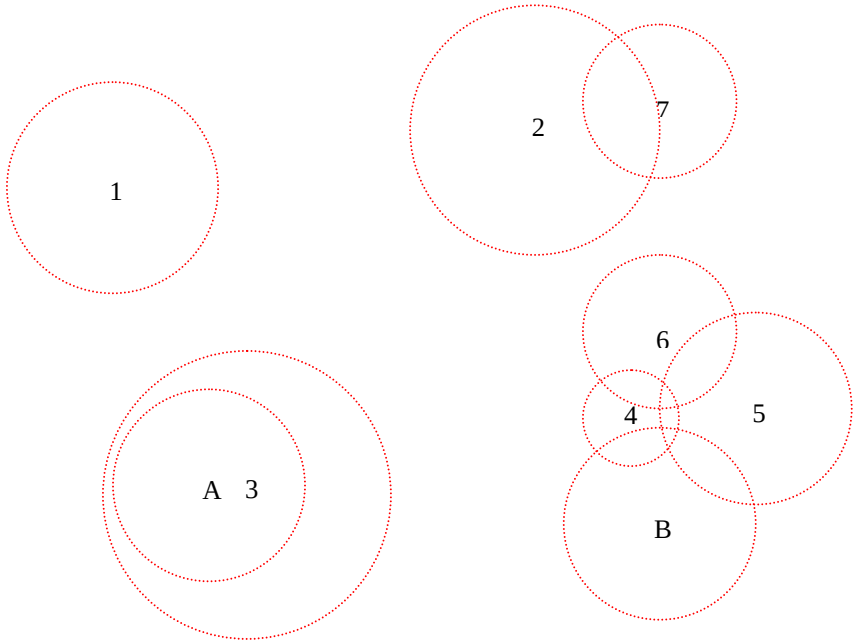


Figure 7. A scenario with nine sites.

Each of the circles is named using a single letter or number such as 1, 2, 3 or A, B, C etc which represents their respective weapon system symbol. It is important to use a single letter or number to represent each circle to avoid confusion when there are overlapping circles. Next we check for intersecting circles. One computationally efficient

way to do so is to enclose each and every circle using a square, because it is faster to check the intersection between squares than circles.

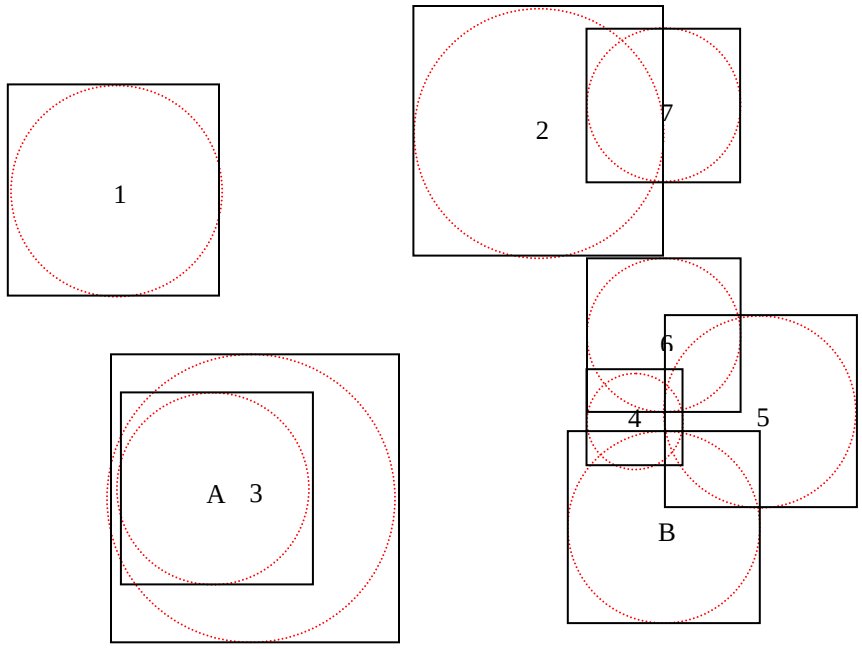


Figure 8. Surrounding circle with square.

The squares are checked to see if the intersection is affirmative. We then proceed to check if the circles really intersect by using Equation 2.1.

$$R_i + R_j \leq \sqrt{(X_i^2 - X_j^2) + (Y_i^2 - Y_j^2)}, \qquad \text{-----(2.1)}$$

where $R_i$ and $R_j$ represent the radii of the respective circles and $X_i$, $X_j$, $Y_i$, and $Y_j$ represent the locations of their centers in Cartesian coodinates.

## B. CONSTRUCTING CLUSTERS

When intersecting circles has been identified, we will group them into clusters. Using two circles for illustration, the possible outcomes are as follows:

a. When the two circles intersect partially, we make the intersection portion invisible and group them as the same cluster

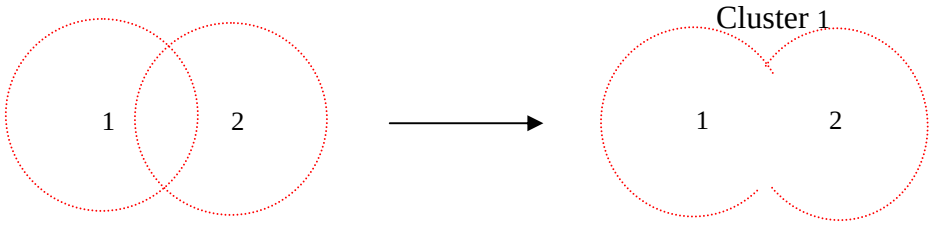


b. When one circle fully enclose the other, we make the inner circle invisible.

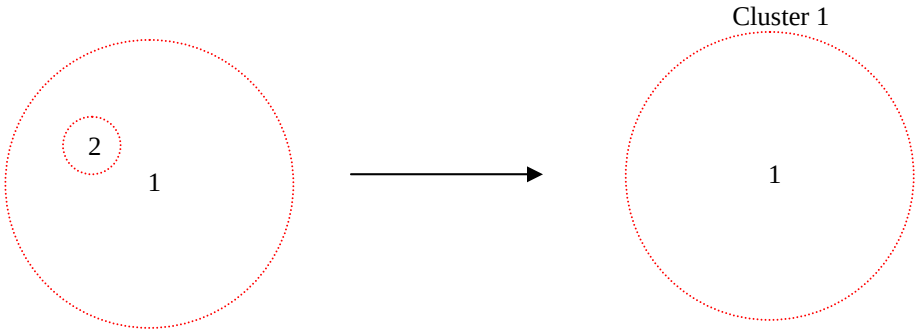


c. When the two circles do not intersect, we group them into separate clusters.

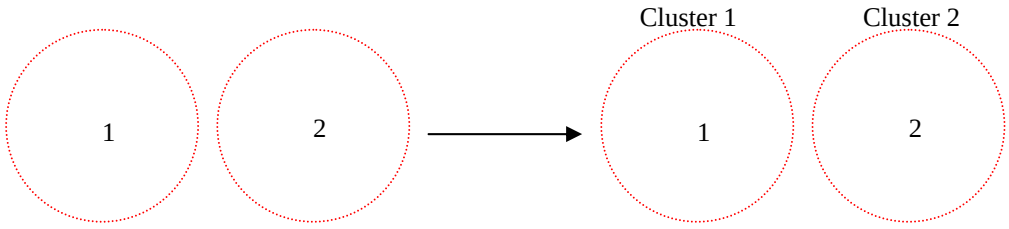


After ‘clusterization’ Figure 7 is represented by Figure 9, where the cluster closest to North is given the lowest number.

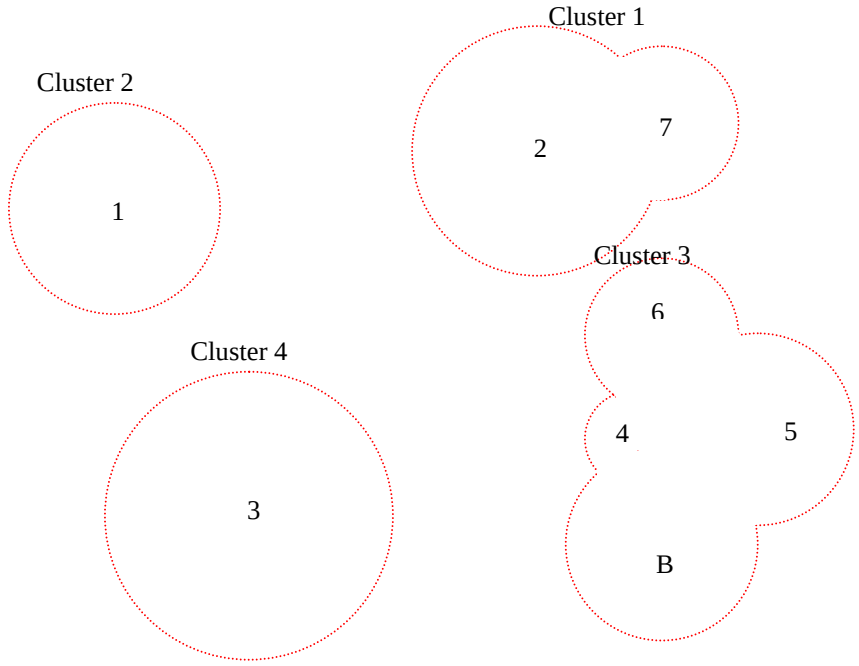


Figure 9. Clusterization of circles.

## C. CONSTRUCTING POLYGONS

When the clusters have been constructed, the arcs of each cluster are approximated using closed polygonal edges. Some of these edges will be used to construct the approximate route, which will be addressed in the next section. We should avoid using short polygonal edges in approximating the clusters' arc because this may cause the optimal route to be made up of too many short edges, hence resulting in maneuvering difficulty. Having too many short edges in the optimal route also degrades computation time.

Figure 10 shows the construction of polygonal edges surrounding each cluster. Each polygonal edge is tangential to the cluster at at least one point and the number of polygonal edges used depends on the radius of the kill envelope.

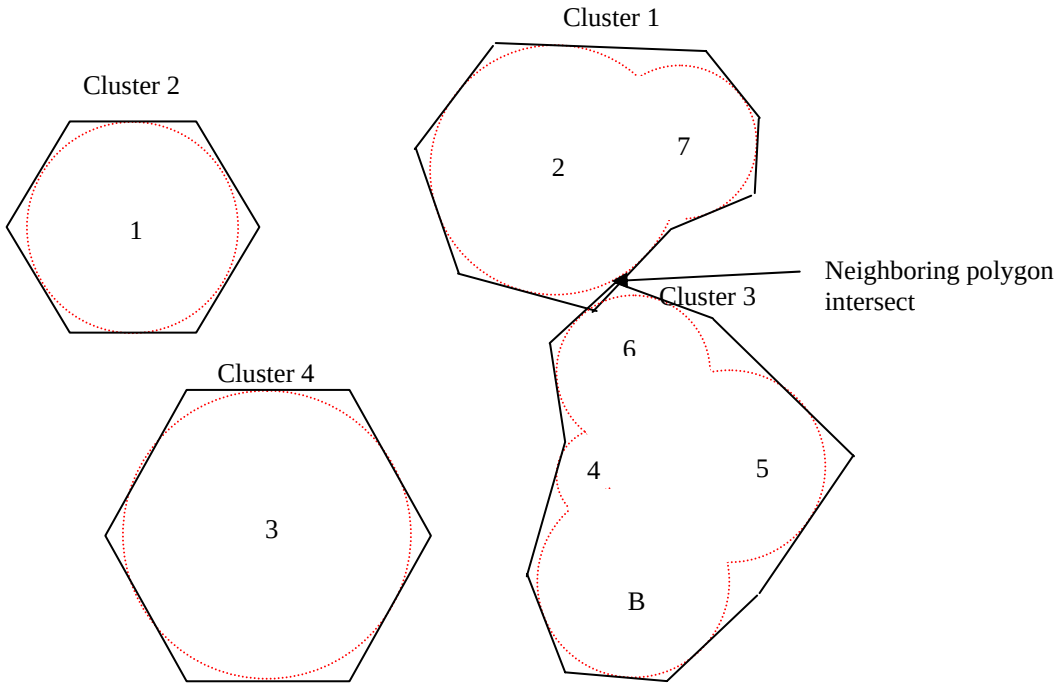


Figure 10. Construction of enclosing polygons.

After constructing the enclosing polygon, we need to check if neighboring polygons intersect. In Figure 11, the polygon enclosing cluster 1 intersects the polygon enclosing cluster 3. In such a case, we need to perform hewing to disengage the intersecting polygons. This can be done by adding an extra edge to one of the polygon or to both of the polygons, depending on the depth of intersection.

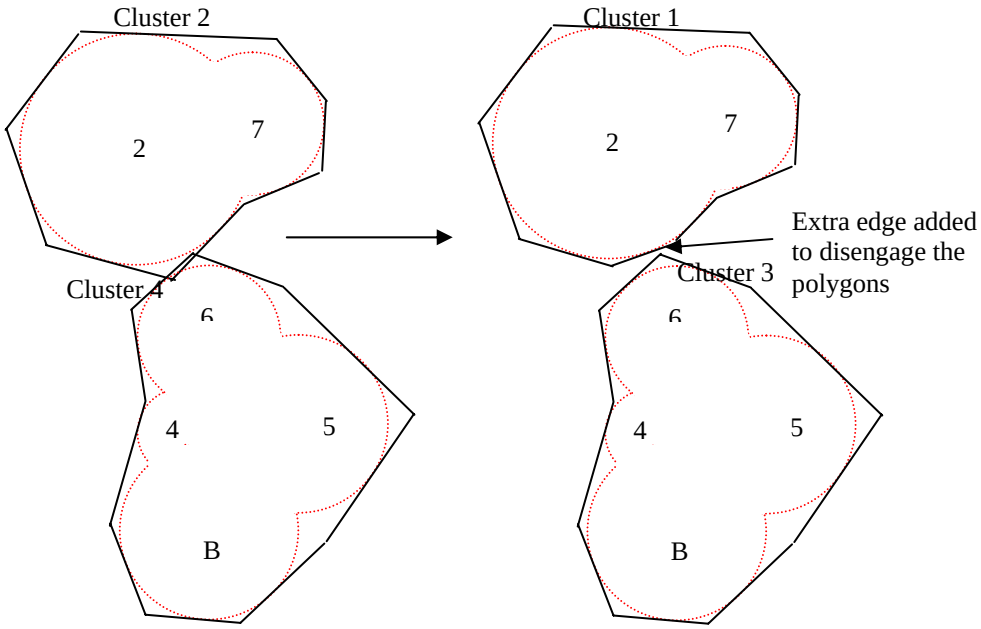


Figure 11. The clusters after hewing and disengaging.

## D. APPROXIMATE ROUTE CONSTRUCTION

The objective of this process is to construct an approximate route, which avoids encroaching into any known surface-to-air weapon kill envelopes from the current aircraft's location to its pre-selected destination.

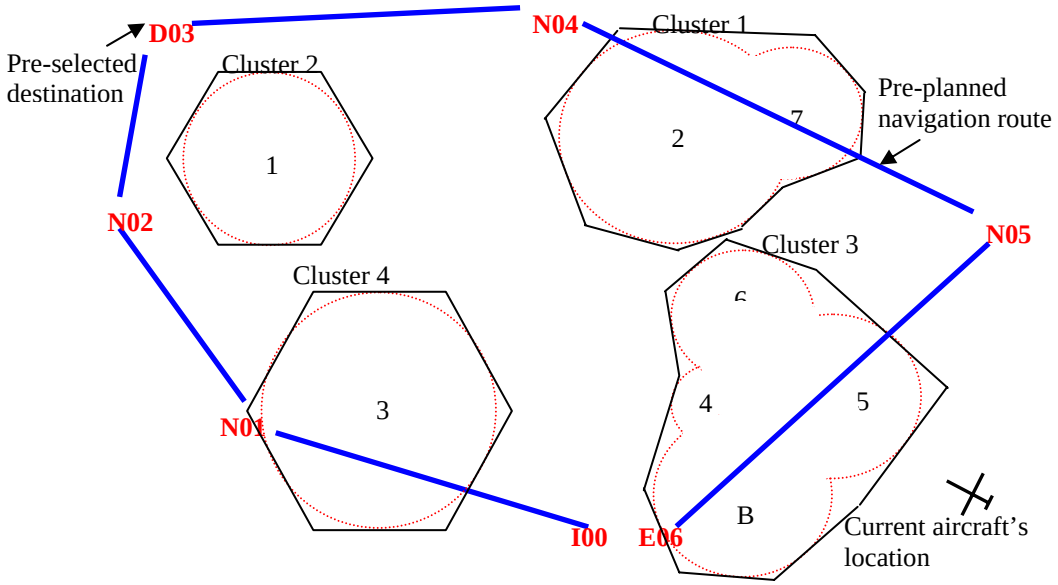


Figure 12. The current location of the aircraft and its pre-selected destination (D03).

The solid blue line in Figure 12 is the pre-selected navigation route and the labels such as I00, N01 etc. are the navigation waypoints. I represent initial, N represents navigation, D represents destination and E represents end.

Using the current aircraft location as a start point, a straight line is constructed to its destination, which is the end point. The portions of this straight line which intersect the polygons are indicated as dotted lines and they will be checked to see if they intersect the clusters.

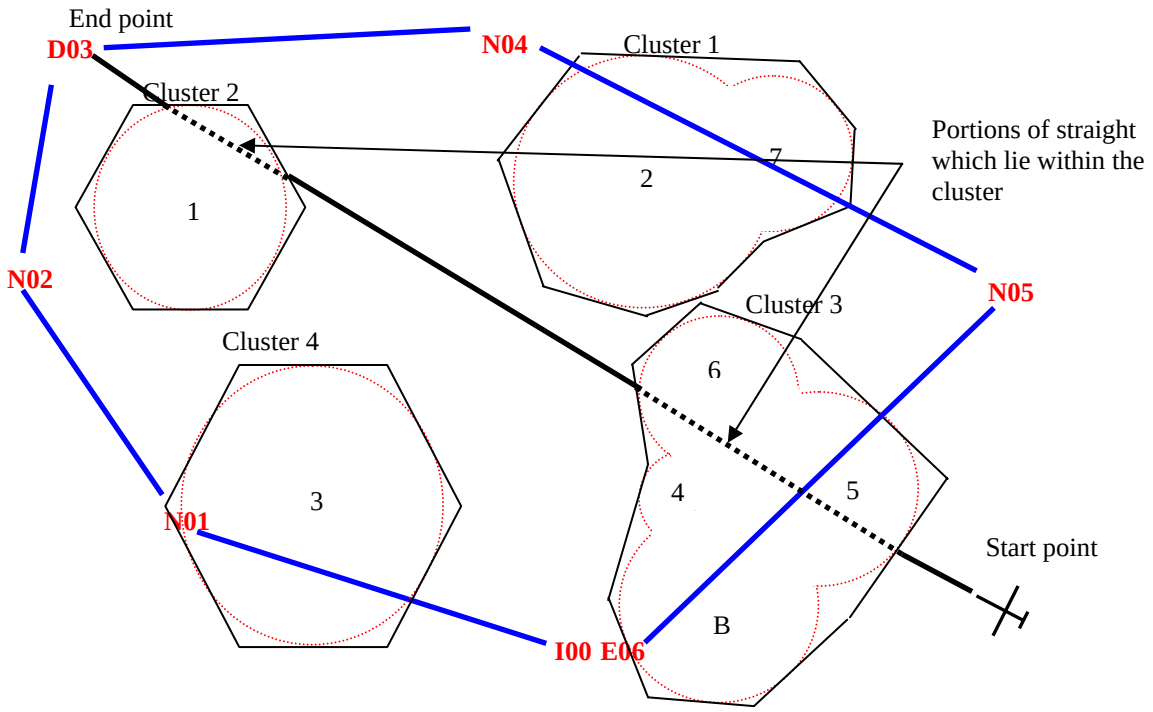


Figure 13. The construction of a straight line from start to end point.

Figure 13 shows that the straight line constructed from the start to end point intersected cluster 2 and 3. The dotted lines, which lie within the cluster, will be re-routed using the polygonal edges. It is important to note that the straight line should have an even number of intersection points with the polygons. The first intersection point is called the entry point and the next is called exit point and so on.

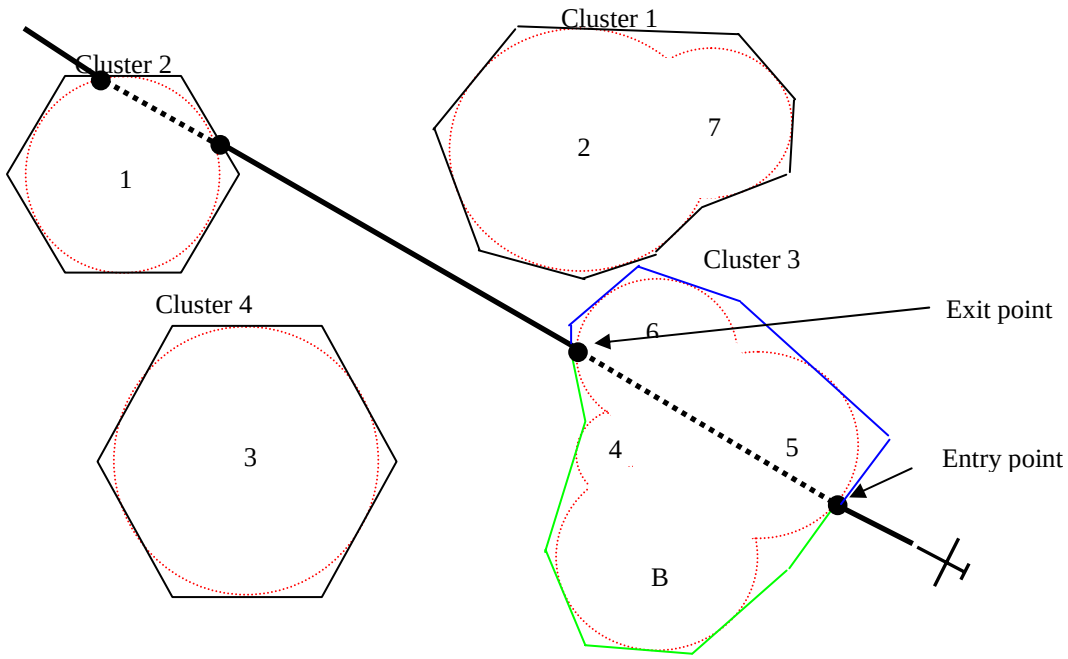


Figure 14. The entry and exit points.

Figure 14 shows the entry and exit points for cluster 3. There are two options available to re-route the dotted line from the entry to exit point. The blue lines indicate option 1 and the green lines indicate option 2. The distances of both these options are computed and the one with the shorter distant is used for re-routing. The same process is applied for cluster 2. Figure 15 shows the resulting approximated route.

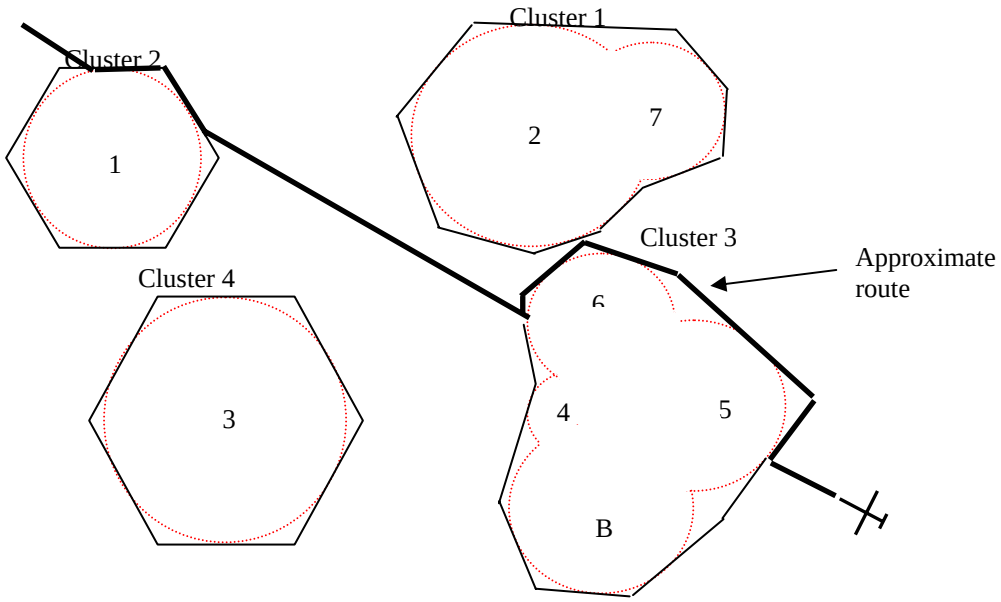


Figure 15. The construction of an approximate route.

## E. DELABYRINTHIZATION OF THE APPROXIMATE ROUTE

From this point onwards the intersection of each segment in the route will be called a vertex. Delabyrinthization is a process to make the approximate route shorter by eliminating some of the vertices, if possible. It can be achieved by the following:

a. For each route vertex, starting from the second vertex[2], remove that vertex and join the previous vertex to the next vertex.

b. Check that the new line constructed does not intersect any kill envelopes. If the check fails, keep that vertex and move on to the next vertex until the second to last vertex is reached. Otherwise, eliminate that vertex.

## F. ROUTE DYNAMIC PROGRAMMING

The word programming in the name has nothing to do with writing computer programs. Mathematicians use the word to describe a set of rules, which anyone can follow to solve a problem. They do not have to be written in a computer language [5].

The general principle of dynamic programming is to `divide and conquer'. The idea is to break a large problem down (if possible) into incremental steps so that, at any given stage, optimal solutions are known to *sub-problems*. When the technique is applicable, this condition can be extended incrementally without having to alter previously computed optimal solutions to sub-problems. Eventually the condition applies to all of the data and, if the formulation is correct, this together with the fact that nothing remains untreated gives the desired answer to the complete problem.

In fact, the route dynamic programming can be viewed as this principle taken to extremes. If it is not possible to work out exactly how to divide up a problem into smaller problems, it is sometimes worth taking the approach of solving all the smaller problems, and storing them away to be combined and used when solving the larger problem. This idea is illustrated by the optimal path algorithm, which we will address in this section.

[2] Delabyrinthization is not applicable to the aircraft current location and destination since they cannot be removed.

Prior to applying this technique, a method for reducing the number of legs by variations in the vertices must be introduced.

## G. LEG REDUCTION THROUGH THE METHOD OF VARIATIONS

The first objective of this process is to provide a set of small possible variations for each of the vertices in the approximate route. The set of variations for each vertex are called “candidate” vertices.

For each variable vertex, four candidate vertices at a small distance from the original vertex are generated. Each candidate vertex is checked for kill envelope avoidance, and it is excluded from the set if it is found to lie within any kill envelope. Figure 16 shows the result of the variations. The original vertices are indicated with empty dots and their candidates are indicated by filled dots. Those vertices, which lie within the kill envelope, have been excluded in the diagram.

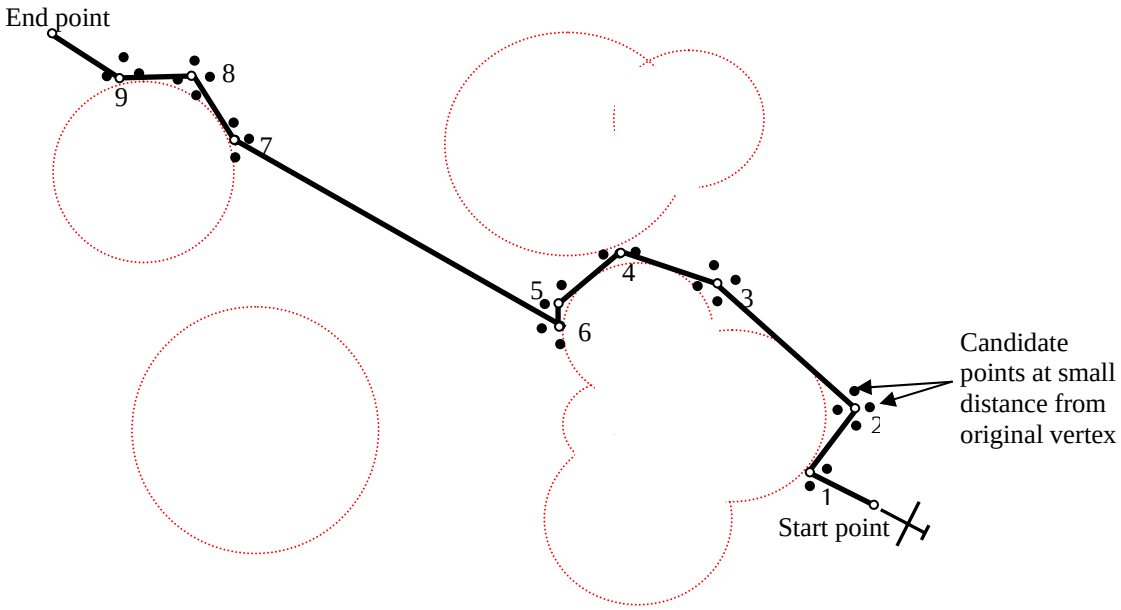


Figure 16. The construction of variations in the vertices used to determine the optimal route.

The second objective of this process is to try to unify two consecutive leg segments of the route into one. The simplest way to do this is the elimination of vertices from the route. The resulting unified segment is checked for kill envelope avoidance. If the unified segment is found to intersect any kill envelope, it is thrown out. Figure 17 shows the result of the elimination where vertices 1 and 6 have been eliminated from the approximate route.

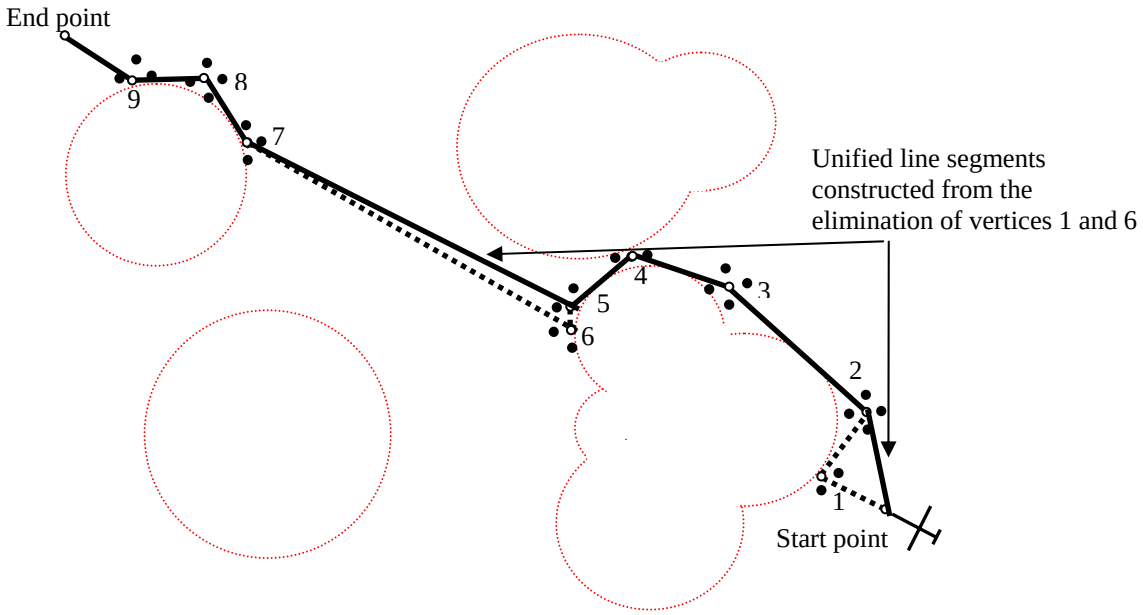


Figure 17. Leg reduction process used to delete vertices 1 and 6.

## H. SEARCH FOR AN OPTIMAL ROUTE

The distance of the entire route can be computed by summing up the length of each line segment that is formed by each consecutive pair of vertices using the merit function equation.

$$\text{Merit function} = \sqrt{(X_i^2 - X_j^2) + (Y_i^2 - Y_j^2)} \qquad \text{-----(2.2)}$$

$$\text{Total route length} = \sum_{i}^{N} lines\ segment_i \qquad \text{-----(2.3)}$$

The objective is to apply route dynamic programming repeatedly until the shortest route distance is found [1]. In each iterative process, each vertex is checked for possible

elimination. Odd numbered vertices are checked first followed by even numbered vertices in the next iteration, and so on. Figure 18 and Figure 19 show the results.

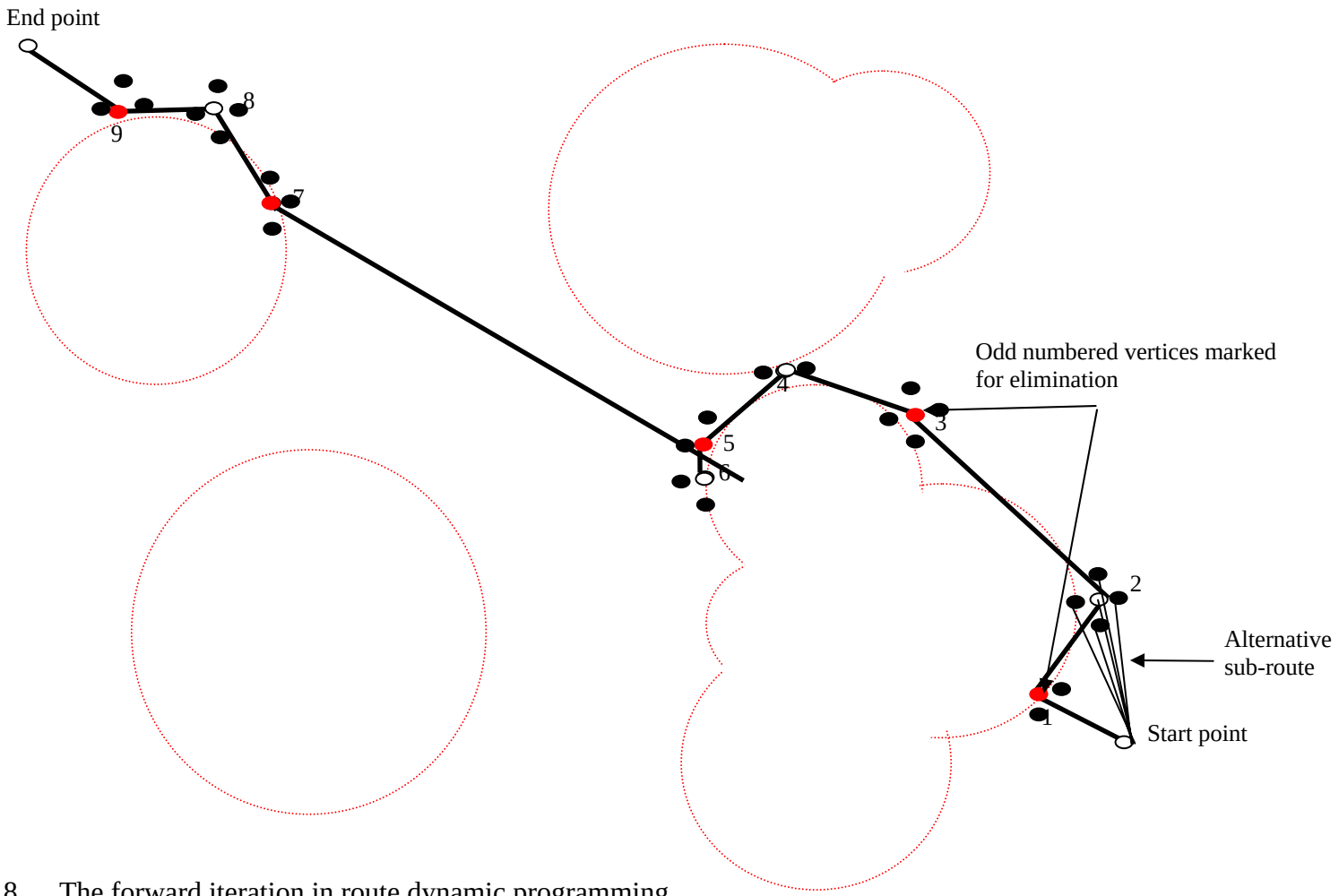


Figure 18. The forward iteration in route dynamic programming.

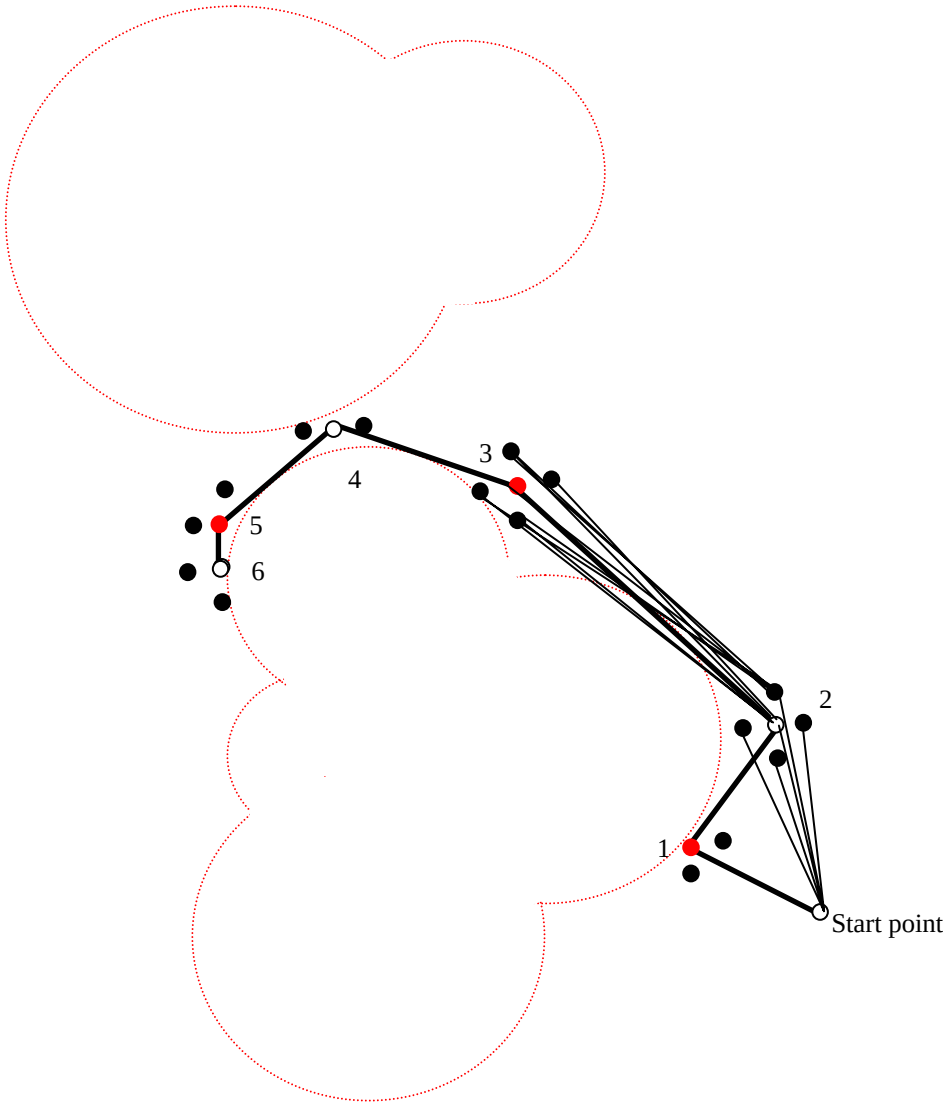


Figure 19. A magnification of the first part of the route.

In Figure 19, the vertices marked for possible elimination are indicated by filled red dots. Beginning from the start point, alternative line segments are constructed from the start point to each and every candidate vertex formed by the leg reduction process in vertex 2.

Figure 19 is a magnification of the first part of Figure 18. It shows the alternative line segments constructed from vertex 2 to the candidate points of vertex 3. To avoid cluttering, only line segments constructed from one of the candidate points of vertex 2 to all candidate points of vertex 3 are shown.

Alternative sub-routes are constructed to all vertex 3 candidates even though vertex 3 is marked for elimination, because there is no possible sub-route from vertex 2 to vertex 4 which avoid kill envelopes. All possible sub-routes which avoid kill envelopes and which join the start point to the end point are listed and this process is repeated till the end point.

Beginning from the start point, every sub-route distance that joins the start point to all candidate points of vertex 2 are computed and stored. The candidate point that has the shortest distance is marked as the best candidate. Continuing from vertex 2, all sub-route distances from its candidate points to all candidate points of vertex 3 are computed and stored. Each of these sub-route distances from candidates of vertex 2 to candidates of vertex 3 is computed and added to the previous sub-route distances computed and stored from the start point.

This process is continued till the end point. At every vertex visited, its sub-route distance and its partial sum of the sub-route distances are computed and stored.

When the end point is reached, the shortest distance for this iteration is known. However, the actual line segments that combine to make up this shortest route are still unknown. The shortest route can be found by back tracking from the end point to the start point. At each vertex, starting from the endpoint, the sub-route that connects the best candidate to the next best candidate is chosen until the start point is reached.

The shortest distance and shortest route vertices for this iteration is stored. The entire above process starting from the forward iteration is repeated with the even

numbered vertices marked for elimination. The result obtained from this iteration is compared with the previous and the better of the two results is stored. The iteration stops when the route distance converges.

Figure 20 shows the shortest route for this example. The number of iterations required to find the shortest route greatly depends on the number of kill envelopes and their geometric orientations.

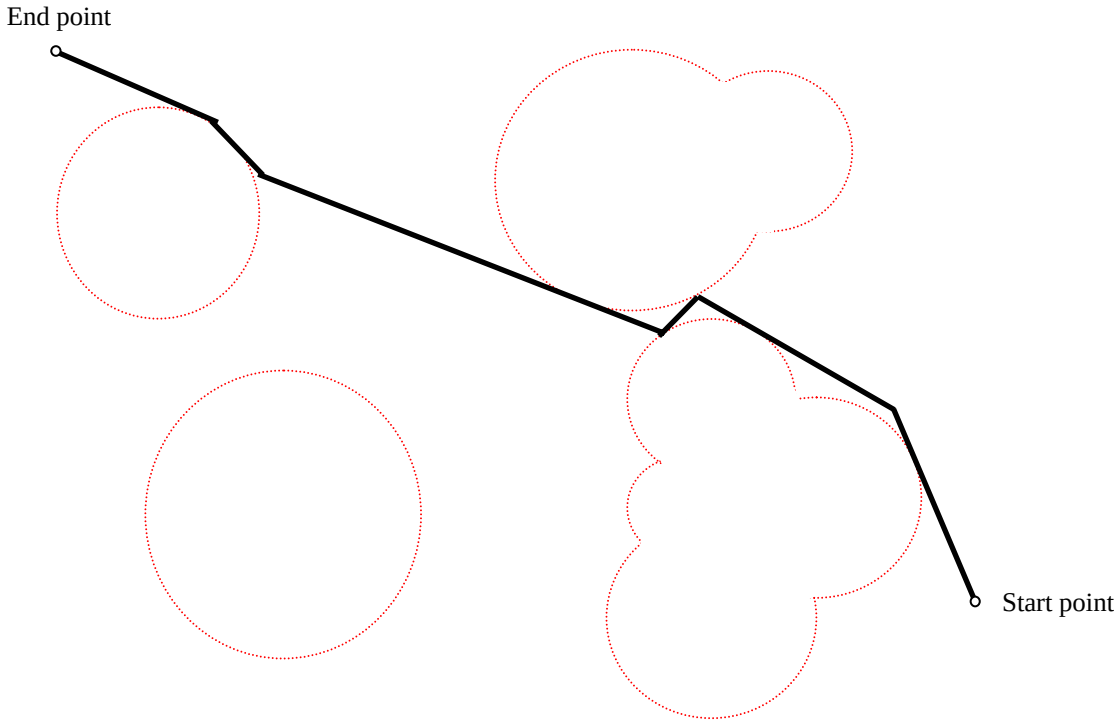


Figure 20. The computed optimal route.

## I. SMOOTHING SHARP TURN EDGES

Sharp turn edges in the optimal route are undesirable since they cannot be executed easily. Therefore, the aircraft will need to use ‘turn arcs’ to smooth out sharp edges whenever possible. The radius of the turn arc is computed using Equation 2.4.

$$R = \frac{V}{g \tan \vartheta}, \qquad \text{-----(2.4)}$$

where R represents the turn arc radius, V represents speed of the airborne vehicle, g represents acceleration due to gravitational force and θ represents roll angle of the airborne vehicle.

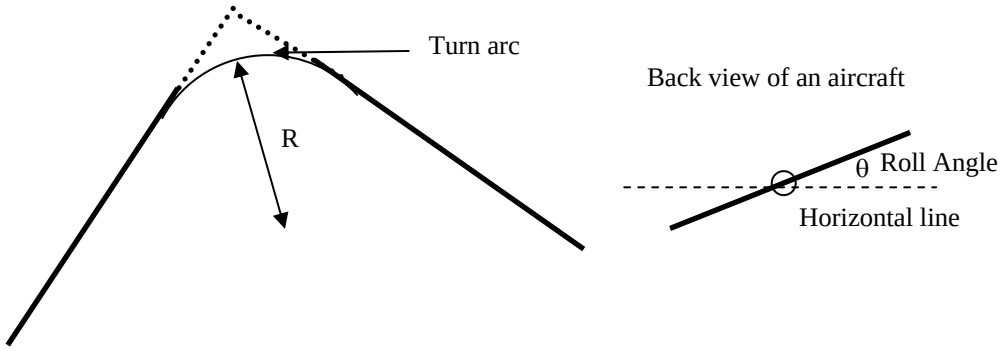


Figure 21. Illustration of a turn arc inserted to smooth out sharp edge formed between two lines and the roll angle of an aircraft.

## J. SCENARIOS

The following sections illustrate examples which require fine tuning of the optimal route algorithms so that it can function properly. The dynamic behavior of the optimal route algorithms will be illustrated with examples at the end of this chapter.

## K. BOUNDARY CASES

In section II D (**APPROXIMATE ROUTE CONSTRUCTION**) of this chapter, it was mentioned that the re-routing mechanism requires the straight line to have an even number of intersection points with polygons surrounding the clusters. One scenario which fail this requirement is when the airborne vehicle falls inside the polygon but outside the cluster. Figure 22 shows the scenario.

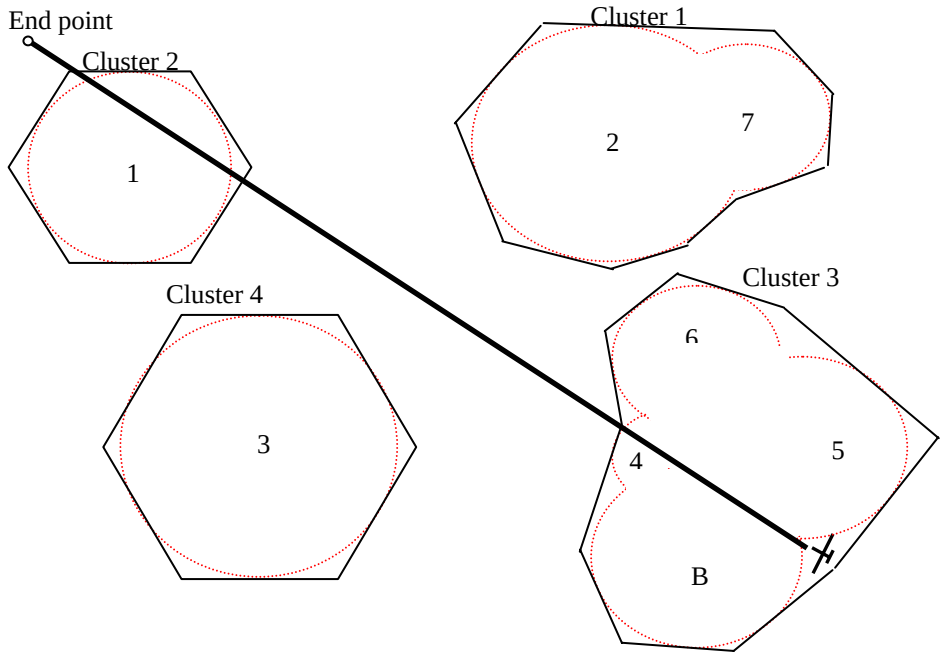


Figure 22. Start point of aircraft falls in polygon but not in kill envelope.

The straight line constructed intersects the polygon of cluster 3 but only one intersection can be found. The algorithms treat this as an entry point and will search fruitlessly for the exit point. To overcome this, the aircraft has to be checked to see if it falls inside any polygon before constructing the straight line.

An efficient method to do this is to construct an infinitely lone vertical or horizontal line from the aircraft location and check the number of times this line intersect the polygons constructed [1]. Odd numbers of intersections conclude that the aircraft is within a polygon and even numbers conclude the other. Figure 23 shows the validity check.

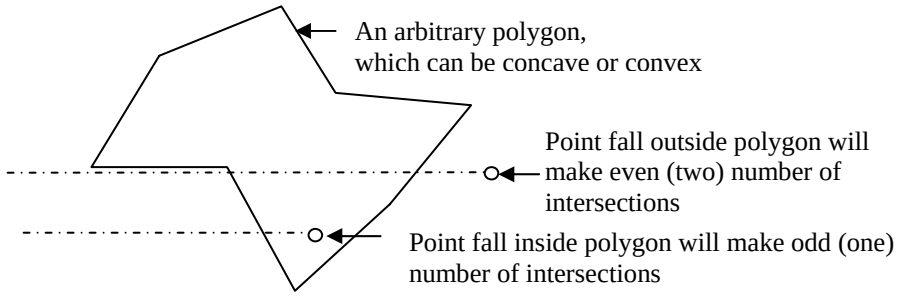


Figure 23. The check of whether a point falls outside or inside a closed polygon.

If the aircraft falls inside the polygon, additional edges are constructed to exclude the aircraft. Figure 24 shows the result.

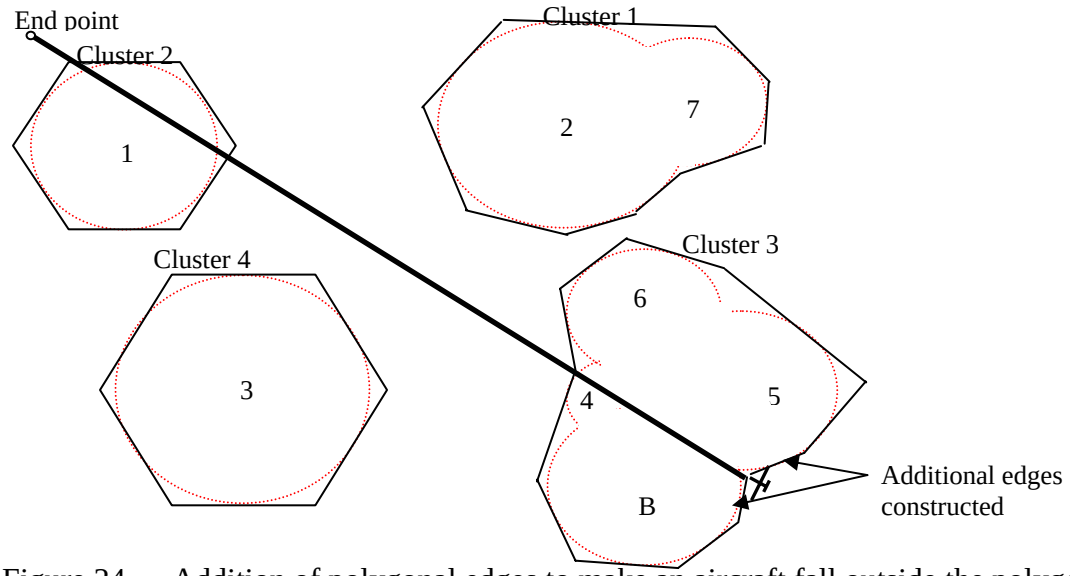


Figure 24. Addition of polygonal edges to make an aircraft fall outside the polygon.

There is no solution when the aircraft inside a cluster. It is assumed that if the aircraft finds itself within a kill envelope, it will exit in the most expeditious fashion. A solution can be implemented if the end point falls inside a cluster, but will not be addressed in this thesis. Figure 25 and Figure 26 shows the scenario.

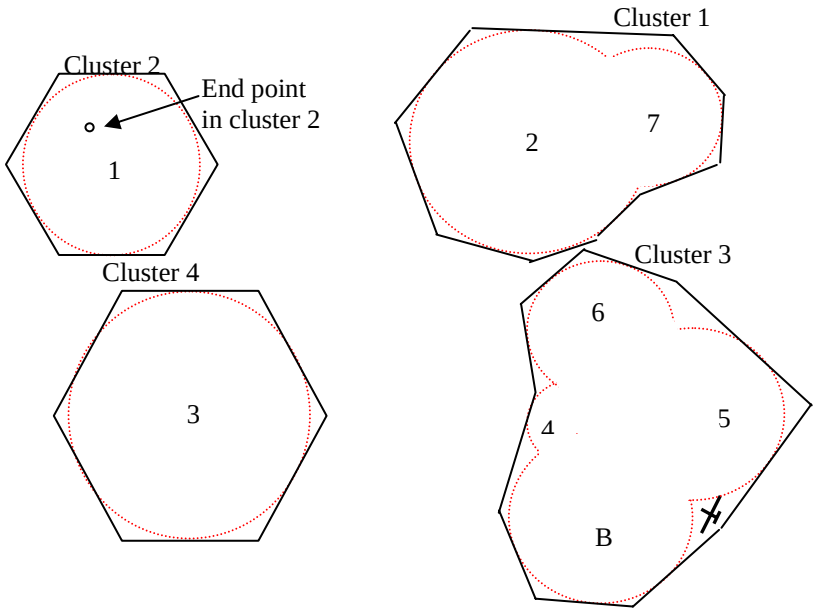


Figure 25. An example in which the end point falls inside a kill envelope.

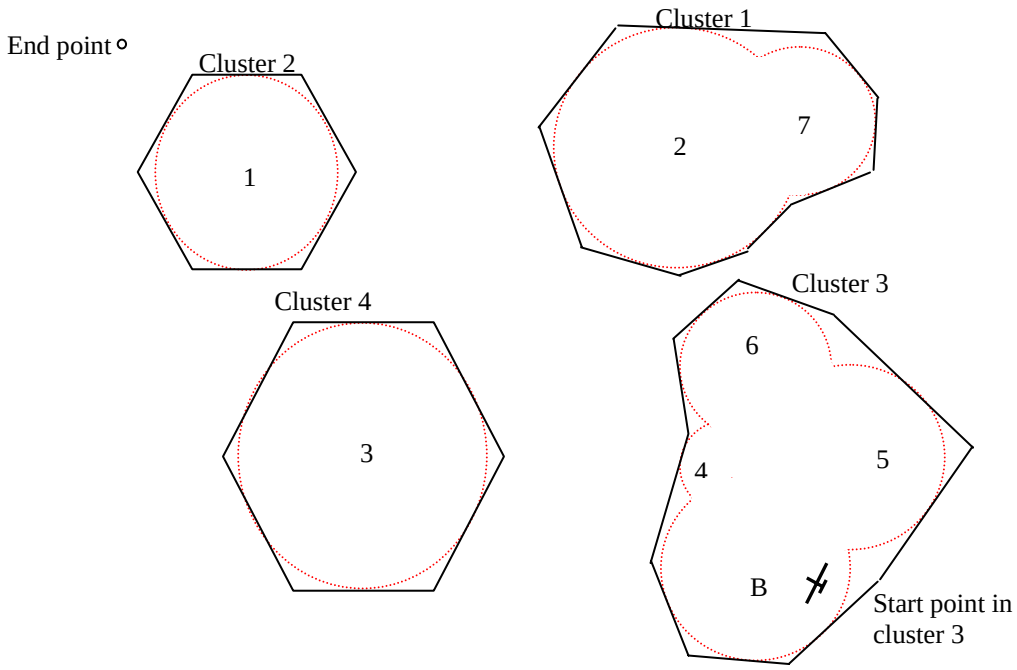


Figure 26. An example in which the start point falls inside a kill envelope

## L. DYNAMIC BEHAVIOR OF THE OPTIMAL ROUTE

The software routine responsible for activating the route dynamic programming is also responsible for the dynamic behavior of the optimal route [1]. This routine continues to activate the route dynamic programming algorithms even after the optimal route is found. It constantly checks and make sure that the optimal route is still valid when there is a geometric change in the combat area, which could be due to site update, a new site is formed in real time or when the aircraft changes its altitude.

When the optimal route is found to be invalid, this software routine will attempt to amend or fine-tune a portion of the route, instead of re-computing a new route from the beginning. A re-computation is activated only if the fine-tuning algorithm fails to fix the problem. The objective of fine-tuning the route, instead of a re-computation is to make the algorithm more efficient. Figure 27 and Figure 28 illustrates the methods employed for fine-tuning the optimal route. All amended sub-routes have to be checked for kill envelope avoidance.

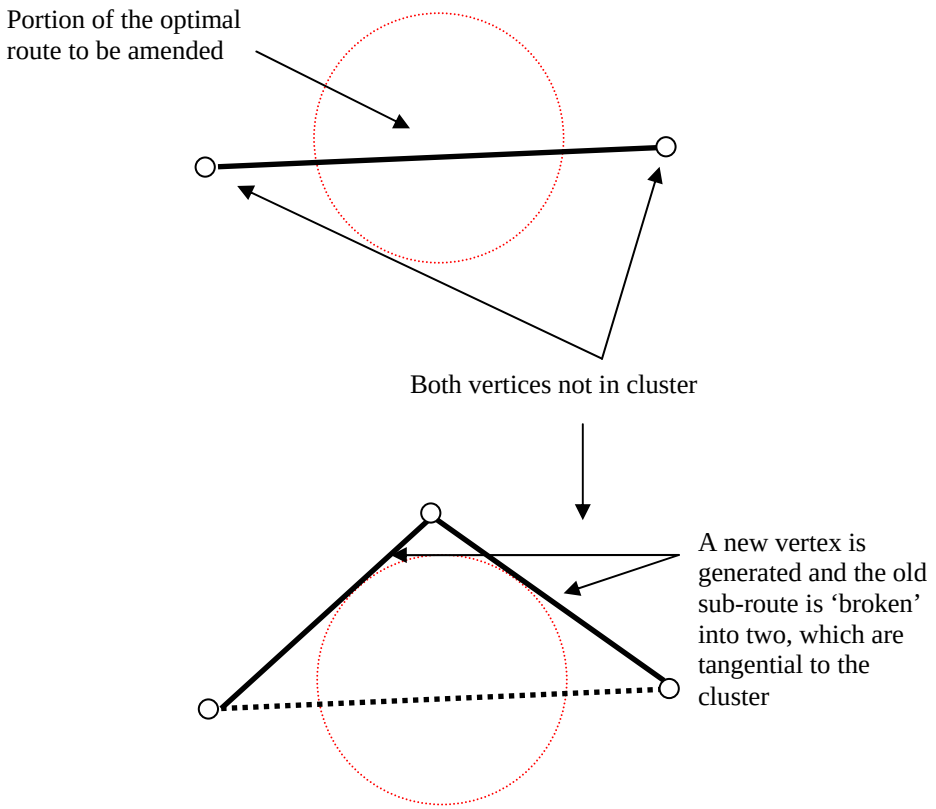


Figure 27. A method to move a leg of the route out of the kill envelope when none of the vertices fall inside the kill envelope.

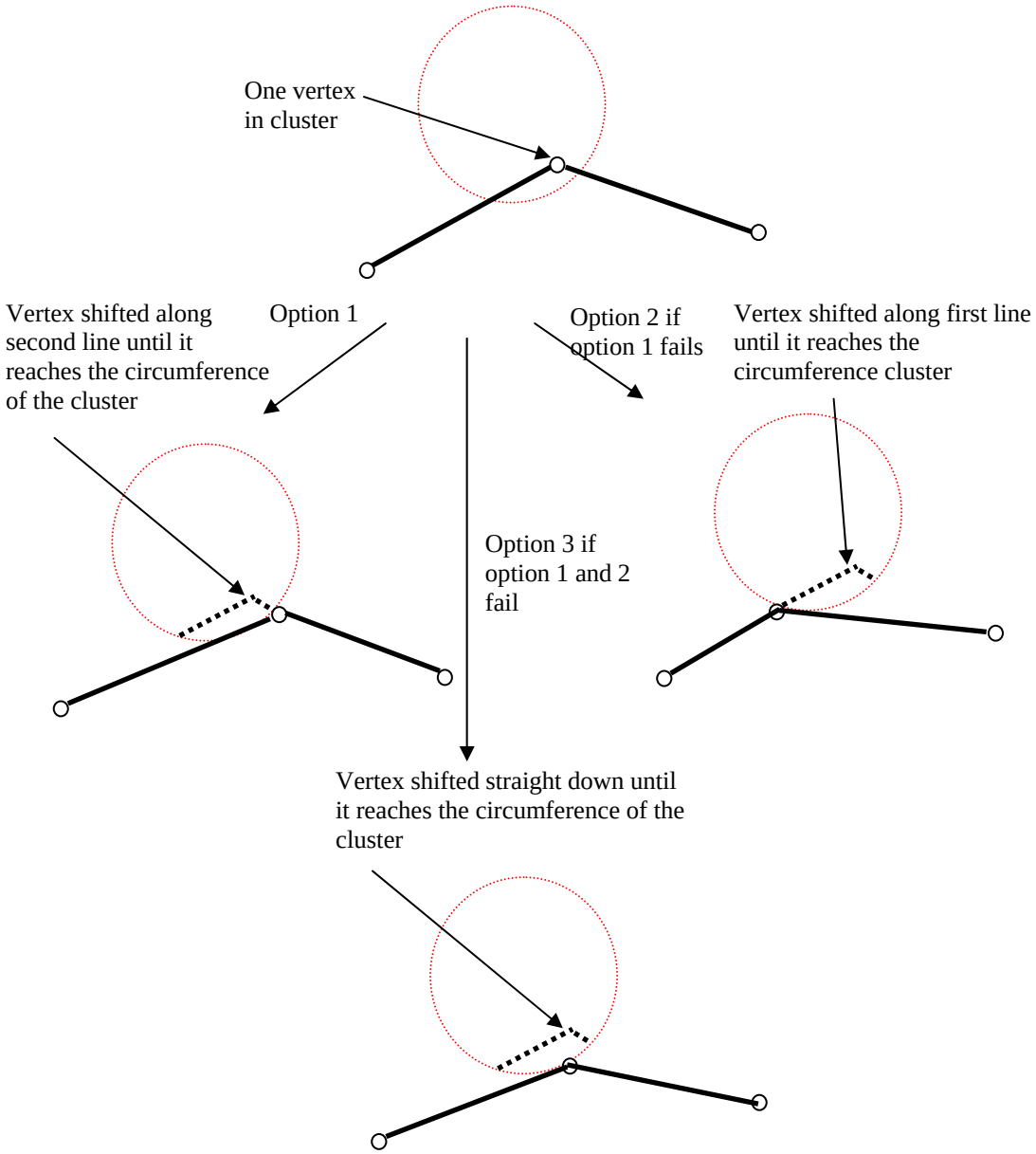


Figure 28. A few methods of shifting the vertices out of the kill envelopes.

Figures 29 and Figure 30 show examples of fine-tuning the route while Figures 30 and 31 show examples of re-computing of the entire route. In the case of fine-tuning, the start point of the optimal route is behind the aircraft but in the case of re-computation, the start point of the optimal route is at the current location of the aircraft.

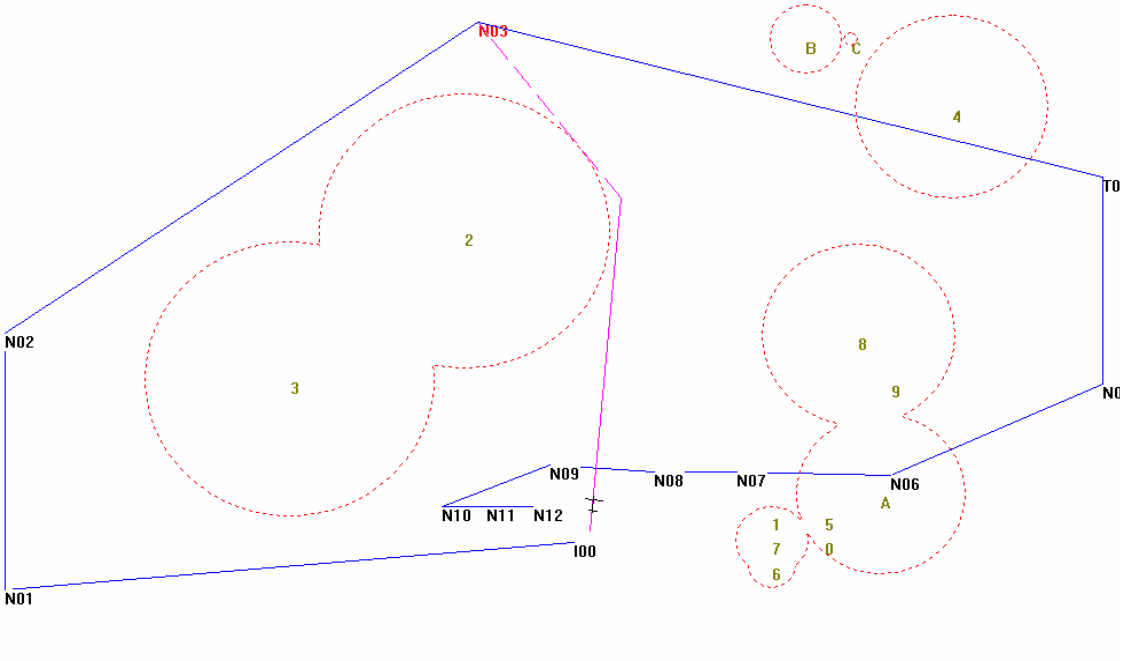


Figure 29. An example of fine tuning the optimal route.

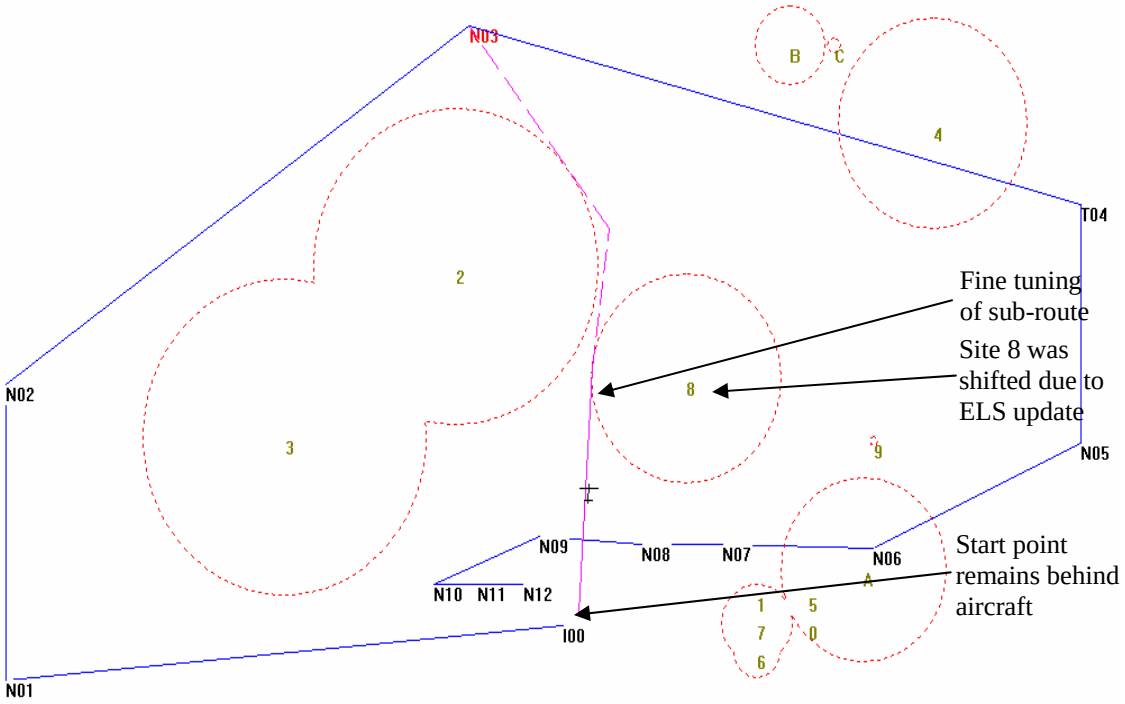


Figure 30. The location updates by ELS caused site 8 to be shifted and intersect the optimal route. Fine tuning process was activated to amend a portion of the route. The start point remains behind the aircraft.

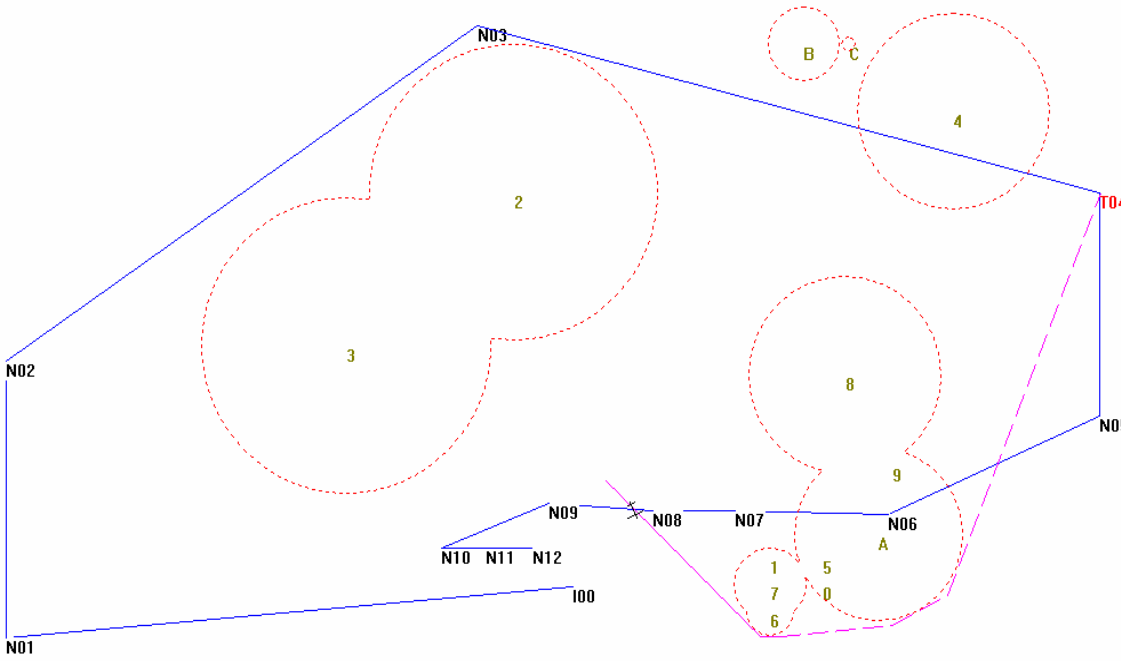


Figure 31. An example that requires a recomputation of the optimal route because fine tuning mechanism fails to amend the route.

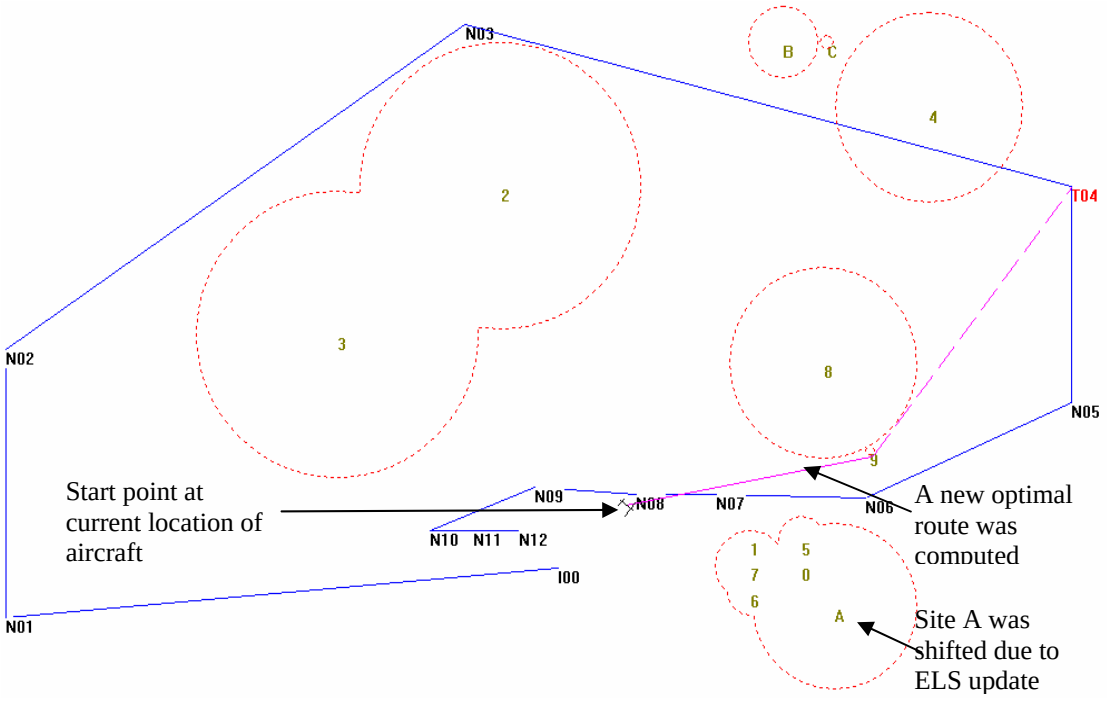


Figure 32. The location update by ELS caused site A to be shifted and intersect the optimal route. Fine tuning process fails to amend the route and the entire route has to be recomputed. The start point is at the current location of the aircraft.

Before closing this chapter, it is worthwhile stating that the sub-route behind the active leg need not be kill envelope avoidance, because it does not endanger the safety of the aircraft. See Figure 33.

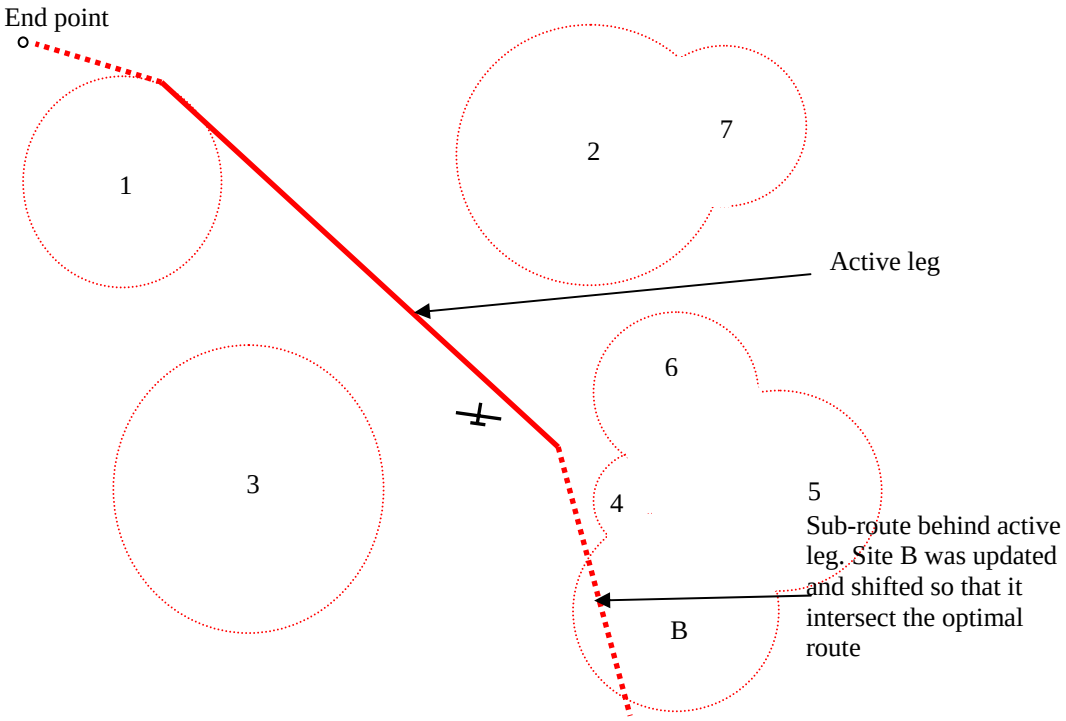


Figure 33. The sub route behind the active leg is not amended.

# III. SPATIAL CORRELATION

The objective of spatial correlation is to establish the probability that the ellipse computed by the emitter locator sensors (ELS) and the preplanned ellipse are the same. Given the ELS uncertainty ellipse, represented by a covariance matrix **R**, and the preplanned uncertainty ellipse, represented by a covariance matrix **P,** the probability of the spatial correlation can be calculated by computing the probabilistic score based on the spatial likelihood function [2].

Figure 34 shows some spatial correlation results for two ellipses. The probabilistic score of the likelihood function must exceed a heuristic threshold value for spatial correlation[3] to be established. To compromise between correlation declaration rate and false alarm rate, a threshold value of 0.15 has been chosen.

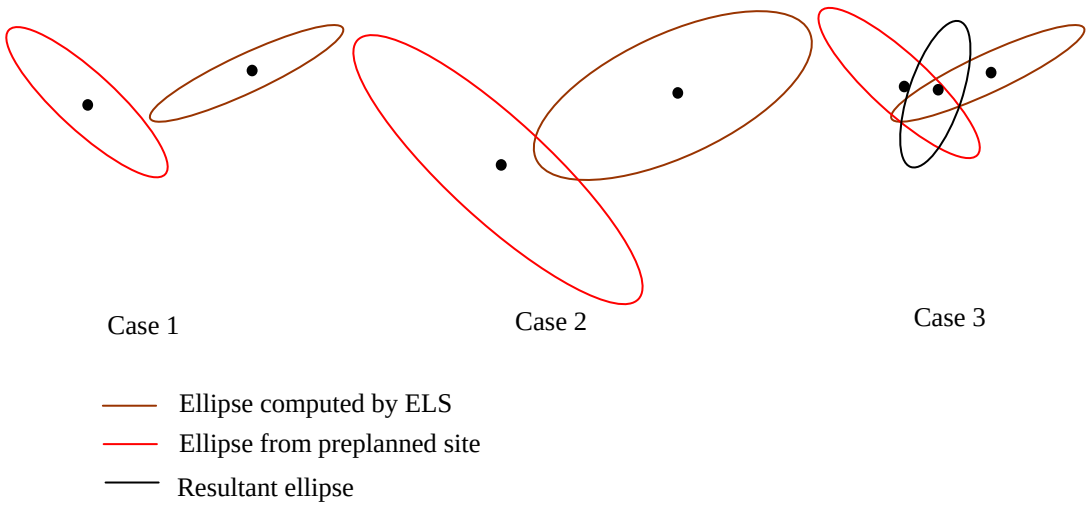


Figure 34. Different correlation results. Cases 1 and 2: No correlation. Case 3: Declared correlation and resultant ellipse.

[3] The threshold number (0 – 1) to establish spatial correlation is arbitrary, but it has to be chosen carefully. If the number is too small, spatial correlation may take a long time to declare correlation. If the number is too large, false correlation may result.

In case 1, the spatial locations of the two ellipses were too far away for correlation to be declared. In this case, the ellipse computed by ELS will form a new site when sufficient measurements have reduced its CEP to approximately 3000 meters. The probability of establishing a correlation beyond this CEP is minimal because the spatial location of the ELS ellipse is relatively accurate.

In case 2, the uncertainties in the covariance matrices of the ellipses are too large for a correlation to be declared. The probabilistic score of the likelihood function does not exceed the threshold value. In this case, more updates from the ELS ellipse is required to reach a decision. A new site is formed when the CEP of the ELS ellipse reaches 3000 meters, if spatial correlation with the preplanned ellipse cannot be declared.

In case 3, the spatial locations and the covariance matrices of the ellipses meet the requirement for correlation to be declared. The probabilistic score of the likelihood function exceeds the threshold value. Hence, the two estimates can be combined to achieve the resultant ellipse.

## A. ELLIPSE COMPUTED BY THE EMITTER LOCATOR SENSORS

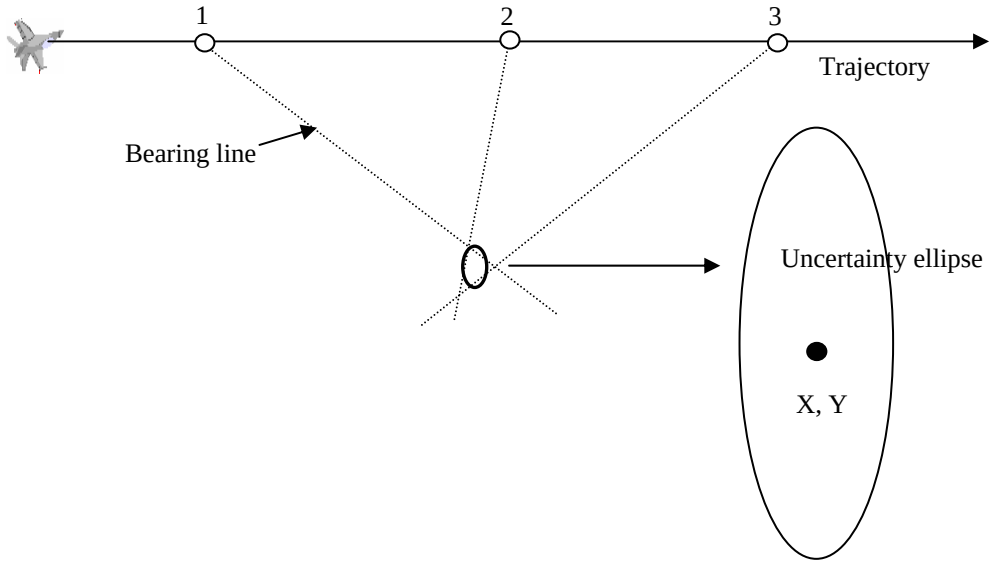


Figure 35. The formation of an ELS ellipse.

Figure 35 shows the formation of the ELS ellipse using the Extended Kalman Filter (EKF) algorithm [2]. The CEP of the ellipse can be calculated by equation 3.1.

$$CEP = A\sqrt{\sigma_1^2 + \sigma_2^2}, \quad \text{-----(3.1)}$$

where $\sigma_1$ and $\sigma_2$ are the eigenvalues of the covariance matrix, representing the uncertainty ellipse, and $0 < A < 1$.

The state vector of a stationary emitter at a particular time can be represented by:

$$\mathbf{x}_k = [x_k \; y_k], \quad \text{-----(3.2)}$$

where $x(k), y(k)$ represent the location of the ground emitter in Cartesian coordinates and $k$ represents time. The output equation of the measurements can be represented by:

$$\mathbf{z}_k(\mathbf{x}) = \mathbf{h}_k(\mathbf{x}) + \boldsymbol{\omega}_k \quad \text{-----(3.3)}$$

Assume that the relative bearings measured by the ELS consist of the elevation angle, θ and azimuth angle, φ.

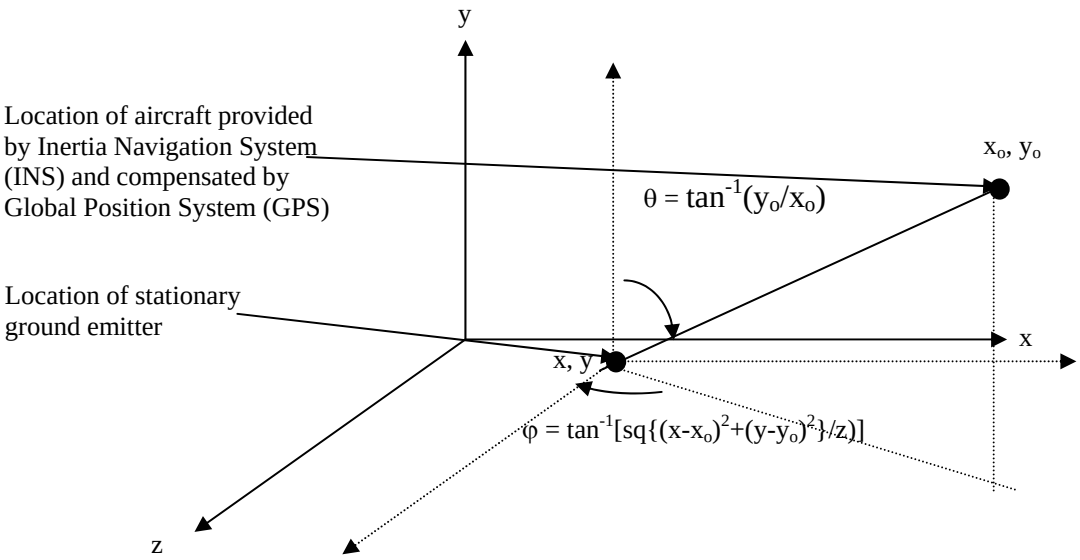


Figure 36. The elevation and azimuth angles of the ground transmitter with respect to the aircraft.

Equation 3.3 can be rewritten as:

$$\mathbf{z}_k(\mathbf{x}) = \mathbf{h}_k(\mathbf{x}) + \boldsymbol{\omega}_k = \begin{bmatrix} \tan^{-1}\left(\dfrac{y - y_o}{x - x_o}\right) \\ \tan^{-1}\left(\dfrac{\sqrt{\{(x-x_o)^2 + (y-y_o)\}^2}}{z}\right) \end{bmatrix}, \qquad \text{-----(3.4)}$$

where the term z in the parenthesis represents the aircraft altitude; it is to be differentiated from the measurement **z**. The term $\boldsymbol{\omega}_k$ in the measurement equation accounts for sensor errors. Hence $\boldsymbol{\omega}_k$ is also known as measurement noise. Assume that the noise term has a normal distribution with zero mean value, and variance **R**, it can be represented by:

$$\boldsymbol{\omega}_k \sim N(0, \mathbf{R}) \qquad \text{-----(3.5)}$$

Assume the ELS has an error of one degree[4] in both the measurements of θ and φ,

$$\mathbf{R} = \begin{bmatrix} \dfrac{1}{3600} & 0 \\ 0 & \dfrac{1}{3600} \end{bmatrix} \qquad \text{-----(3.6)}$$

in which $1^o \approx \dfrac{1}{60}$ radian. Since the ground emitter is stationary, the prediction of the state vector and the covariance matrix are given by:

$$\hat{\mathbf{x}}_{k+1/k} = \hat{\mathbf{x}}_k \qquad \text{-----(3.7)}$$

$$\mathbf{P}_{k+1/k} = \mathbf{P}_{k/k}, \qquad \text{-----(3.8)}$$

respectively, where **P** is a two by two matrix used to determine the uncertainty ellipse. Using the EKF algorithms, the update of the state vector, $\hat{\mathbf{x}}$ and the covariance matrix, **P** at a later time, say *k*+1can be represented by:

$$\hat{\mathbf{x}}_{k+1/k+1} = \hat{\mathbf{x}}_{k+1/k} + K_{k+1}(\mathbf{z}_{k+1} - \mathbf{h}_{k+1}(\hat{\mathbf{x}}_{k+1/k})) \qquad \text{-----(3.9)}$$

[4] Most ELS has the capability of achieving this accuracy. With an error of one degree, the CEP of the uncertainty ellipse can go down to a few hundred meters.

$$\begin{aligned}\mathbf{P}_{k+1/k+1} &= (\mathbf{I} - K_{k+1}\mathbf{H}_{k+1})\mathbf{P}_{k+1/k} \\ &= (\mathbf{I} - K_{k+1}\mathbf{H}_{k+1})\mathbf{P}_{k+1/k}(\mathbf{I} - K_{k+1}\mathbf{H}_{k+1})^T \\ &\quad + K_{k+1}\mathbf{R}_{k+1}K_{k+1}^T,\end{aligned} \qquad \text{-----(3.10)}$$

where the gain term K can be represented by:

$$K_{k+1} = \mathbf{P}_{k+1/k} H_{k+1}^T (\mathbf{H}_{k+1}\mathbf{P}_{k+1/k}\mathbf{H}_{k+1}^T + \mathbf{R}_{k+1})^{-1} \qquad \text{-----(3.11)}$$

The matrix **H** is evaluated by taking the derivative of **h**(**x**) using the best estimate at time k.

$$\begin{aligned}\mathbf{H} &= \left.\frac{\partial \mathbf{h(x)}}{\partial \mathbf{x}}\right|_{\mathbf{x}=\hat{\mathbf{x}}_{k+1/k}} \\ &= \begin{bmatrix} \dfrac{\partial \tan^{-1}(\dfrac{y-y_o}{x-x_o})}{\partial x} & \dfrac{\partial \tan^{-1}(\dfrac{y-y_o}{x-x_o})}{\partial y} \\ \dfrac{\partial \tan^{-1}[\sqrt{\dfrac{\{(x-x_o)^2+(y-y_o)\}^2}{z}}]}{\partial x} & \dfrac{\partial \tan^{-1}[\sqrt{\dfrac{\{(x-x_o)^2+(y-y_o)\}^2}{z}}]}{\partial y} \end{bmatrix} \\ &= \begin{bmatrix} \dfrac{-y+y_o}{\{(x-x_o)^2+(y-y_o)\}^2} & \dfrac{x-x_o}{\{(x-x_o)^2+(y-y_o)\}^2} \\ \dfrac{z(x-x_o)}{\{(x-x_o)^2+(y-y_o)^2)\}^{\frac{3}{2}}} & \dfrac{z(y-y_o)}{\{(x-x_o)^2+(y-y_o)^2)\}^{\frac{3}{2}}} \end{bmatrix}\end{aligned} \qquad \text{-----(3.12)}$$

Substituting **R** (from equation 3.6) and **H** (from equation 3.12) into 3.10 and 3.11, **P** and **H** can be evaluated respectively and hence $\hat{\mathbf{x}}$, which constitute the center of the ellipse can be evaluated[5].

The EKF is initialized from triangulating the first two relative bearing measurements and choosing a large initial covariance.

[5] When **x** is being evaluated, the aircraft location may be updated, hence introducing additional error. But with the availability of the Global Positioning System (GPS) data, the error introduced is negligible compare to $\omega_k$.

## B. ELIMINATION OF AMBIGUOUS BEARINGS

Additional processing is used to eliminate bearings whose errors exceed a certain threshold heuristically defined [1]. When using equation 3.9 and 3.10 to form an initial ELS ellipse, the center of the ellipse can be used as a reference point for comparison and elimination of ambiguous bearings. This indicates that the relative bearings collected by the ELS to form the initial ellipse are extremely crucial.

Using the location of the ELS ellipse and the aircraft, the relative azimuth and elevation angle of the threat to the aircraft can be calculated.

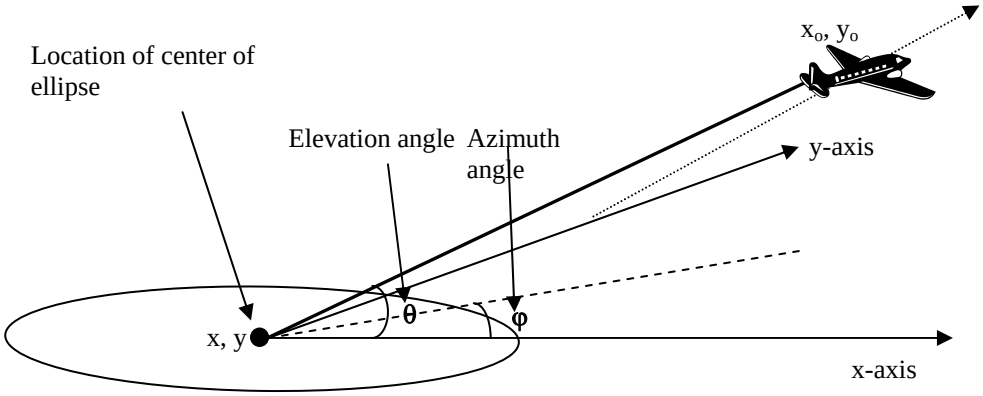


Figure 37. Elevation and azimuth angles.

Figure 37 shows the calculated relative elevation angle, θ and azimuth angle, φ.

θ and φ can be calculated using Equations 3.13 and 3.14 respectively.

$$\vartheta = \tan^{-1}\left(\frac{y - y_o}{x - x_o}\right) \qquad \text{-----(3.13)}$$

$$\varphi = \tan^{-1}\left[\sqrt{\frac{\{(x - x_o)^2 + (y - y_o)\}^2}{z}}\right] \qquad \text{-----(3.14)}$$

The measured relative bearing is compared with the *calculated* ones and if they differ from the threshold by one degree, the measured relative bearing is discarded.

## C. TWO DIMENSIONAL SPATIAL CORRELARION ALGORITHM

The objective of this section is to establish the posterior probability that that the ELS ellipse and the preplanned ellipse belong to the same emitter. Let the center of the ELS ellipse be represented by $\hat{\mathbf{x}}$ (computed using equation 3.9) and its covariance matrix be represented by **P** (computed using equation 3.10). Let the center of the preplanned ellipse be represented by $\hat{\mathbf{y}}$ (known) and its covariance matrix be represented by **R** (known).

Define the difference between $\hat{\mathbf{y}}$ and $\hat{\mathbf{x}}$ to be:

$$\tilde{\mathbf{Z}} = \hat{\mathbf{y}} - \hat{\mathbf{x}} \qquad \text{-----(3.15)}$$

Define the combine covariance of **R** and **P** to be:

$$\tilde{\boldsymbol{\xi}} = \mathbf{R} + \mathbf{P} \qquad \text{-----(3.16)}$$

Define the likelihood function to be [2]:

$$\boldsymbol{\Omega} = \frac{e^{-(\frac{1}{2}\tilde{\mathbf{Z}}^{T}\tilde{\boldsymbol{\xi}}\tilde{\mathbf{Z}})}}{(2\pi)^{1/2}\left|\tilde{\boldsymbol{\xi}}\right|^{1/2}} \qquad \text{-----(3.17)}$$

Define the heuristic correlation threshold value to be:

$$\lambda_o = 0.15 \qquad \text{-----(3.18)}$$

Define the null hypothesis, $H_o$ to be: ELS ellipse correlate with the preplanned ellipse. $H_o$ is accepted when $\boldsymbol{\Omega} \geq \lambda_o$. $H_o$ is rejected otherwise. When $H_o$ is accepted, the two ellipses will merge into one, whereby the situation awareness of the combat environment is improved. However, in cases when there is a false correlation, the survivability of the aircraft may be deteriorated. See Figure 38.

Hence, it is crucial to make the criteria to accept $H_o$ more stringent, as described below.

Define criteria to accept $H_o$ to be: The condition for $\boldsymbol{\Omega} \geq \lambda_o$ must hold for at least five seconds. If the above condition fails to hold when $H_o$ has been accepted before, $H_o$ is rejected immediately, and the two ellipses separate into their respective locations with their respective uncertainty ellipses.

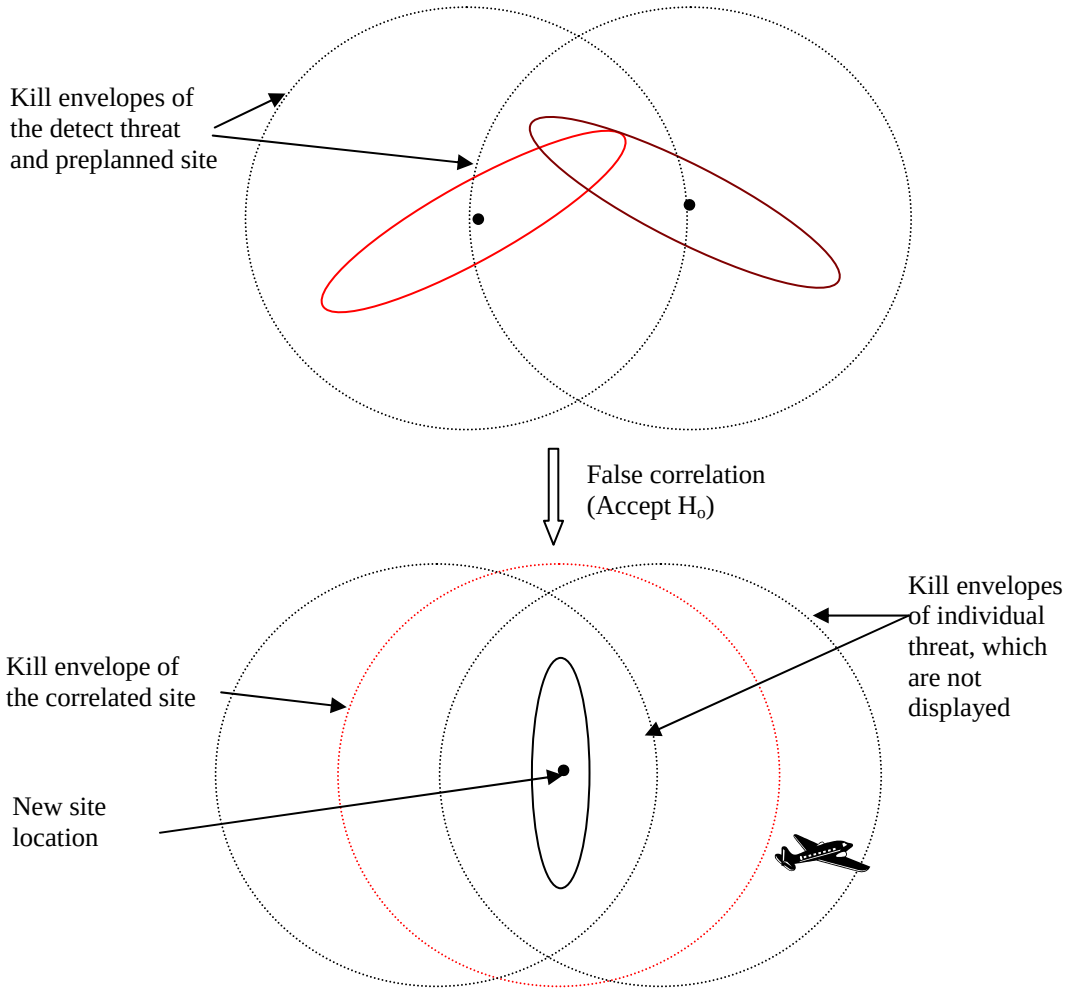


Figure 38. A false correlation occurs and the ELS ellipse merges with the preplanned ellipse. As a result, only one kill envelope is displayed. The aircraft could have penetrated one of the 'real' kill envelopes because they are not displayed separately.

## D. ELLIPSE VERSUS ELLIPSE COMBINATION ALGORITHM

When correlation between the ELS and the preplanned ellipse is established, the resultant ellipse can be computed by combining the two ellipses. Treating the ellipses as multivariate normal estimates of the same location, m [2]:

$$\hat{\mathbf{m}}_1 \sim N(m, \mathbf{R}) \qquad \text{-----(3.19)}$$

$$\hat{\mathbf{m}}_2 \sim N(m, \mathbf{P}), \qquad \text{-----(3.20)}$$

where $\hat{\mathbf{m}}_1$ represents the location and **R** represents the covariance matrix the ELS ellipse and $\hat{\mathbf{m}}_2$ represents the location and **P** represents the covariance matrix of the preplanned ellipse. The location of combined ellipse has distribution represented by:

$$\mathbf{z} \sim N(\hat{\mathbf{m}}, \mathbf{Q}), \qquad \text{-----(3.21)}$$

where

$$\hat{\mathbf{m}} = \mathbf{R}\,[\,\mathbf{P} + \mathbf{R}\,]^{-1}\,\hat{\mathbf{m}}_1 + \mathbf{P}\,[\,\mathbf{P} + \mathbf{R}\,]^{-1}\,\hat{\mathbf{m}}_2 \qquad \text{-----(3.22)}$$

$$\mathbf{Q} = \mathbf{R}\,[\,\mathbf{P} + \mathbf{R}\,]^{1}\,\mathbf{P} \qquad \text{-----(3.23)}$$

See appendix for derivation of equation (3.22) and (3.23).

The materials presented in section III.B, III.C and III.D can be summarized in Figure 38.

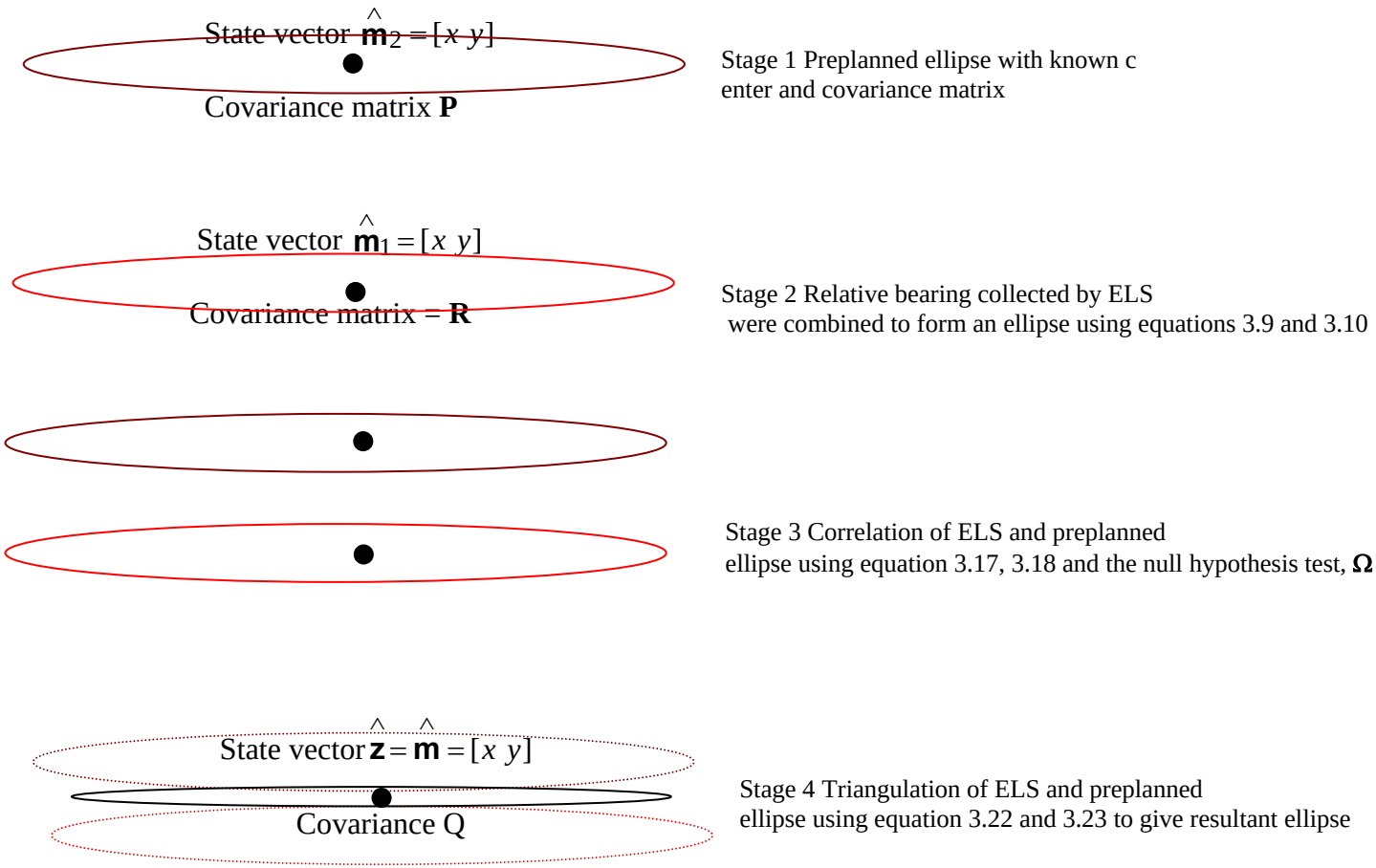


Stage 1 Preplanned ellipse with known c
enter and covariance matrix

Stage 2 Relative bearing collected by ELS
were combined to form an ellipse using equations 3.9 and 3.10

Stage 3 Correlation of ELS and preplanned
ellipse using equation 3.17, 3.18 and the null hypothesis test, $\mathbf{\Omega} \geq \lambda_o$.

Stage 4 Triangulation of ELS and preplanned
ellipse using equation 3.22 and 3.23 to give resultant ellipse

Figure 39. A summary of results

## E. GHOST TARGET ELMINATION

Several factors contribute to Radio frequency (RF) false alarms [1]. For stationary or slow moving targets, ‘ghost’ targets would be most common. ‘Ghost’ targets arise because of the intersection of bearing lines that do not give rise to any real target.

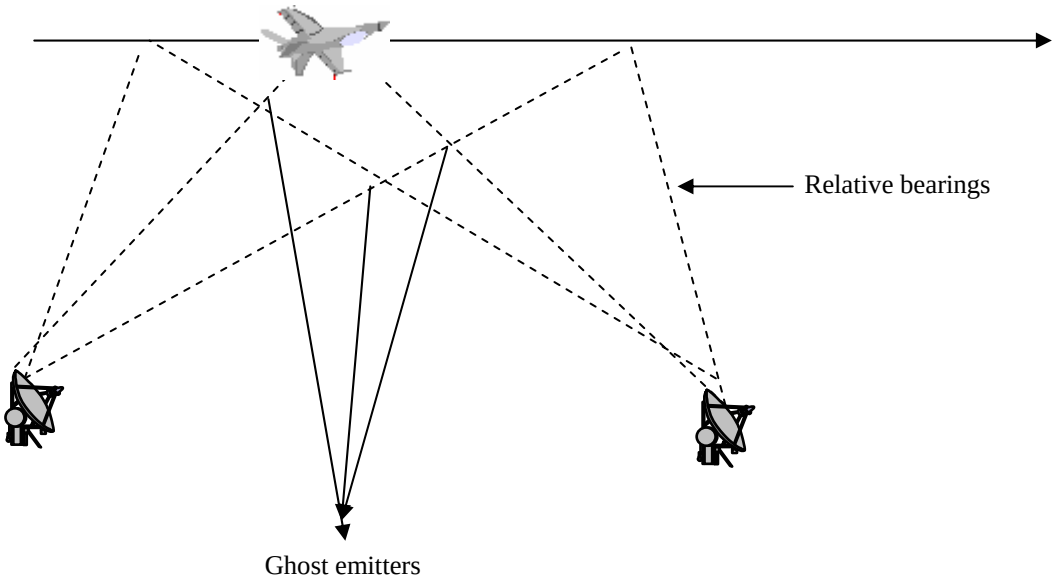


Figure 40. The formation of ‘Ghost’ targets.

The intersection points give rise to ‘ghost’ target. They move together with the platform. But real targets are stationary, hence they can be eliminated. Other sources of flase alarm consist of decoys and beacons which can be differentiated from the real target by means of advanced signal processing techniques.

## F. PREPLANNED SITES AND THREATS LIBRARY

The preplanned data consists mainly of ellipse data, which constitute information of locations of enemy sites prior to sorties [1]. These data can be obtained from Electronic Intelligence (ELINT) Systems [3]. ELINT systems are capable of providing information about the technological status of a potentially hostile environment and about its military activity. This information will have to be translated into plans that can have an impact on the political, military and industrial sphere. ELEINT systems are capable of following the displacement of emitters and provide very accurate Electronic Order of

Battle (EOB) information, which can be loaded into the ELS and mission computers prior to sorties.

The threat library is usually a programmable database [1], which can be uploaded to or downloaded from the ELS or mission computers. It contains information such as, electronic parameters, electronic parameters tolerance, threat types (hopper, switcher, jitter type, etc) of known threats. Upon detection of an active threat, the measured electronic information is used to match the threat library. When a positive match is confirmed, a threat identity (emitter ID or FEID) and a weapon system identity (WSID) are obtained.

Threat libraries cover a very wide scope and in this section, only a subset of it is addressed. Figure 41 shows an example of a typical threat library.

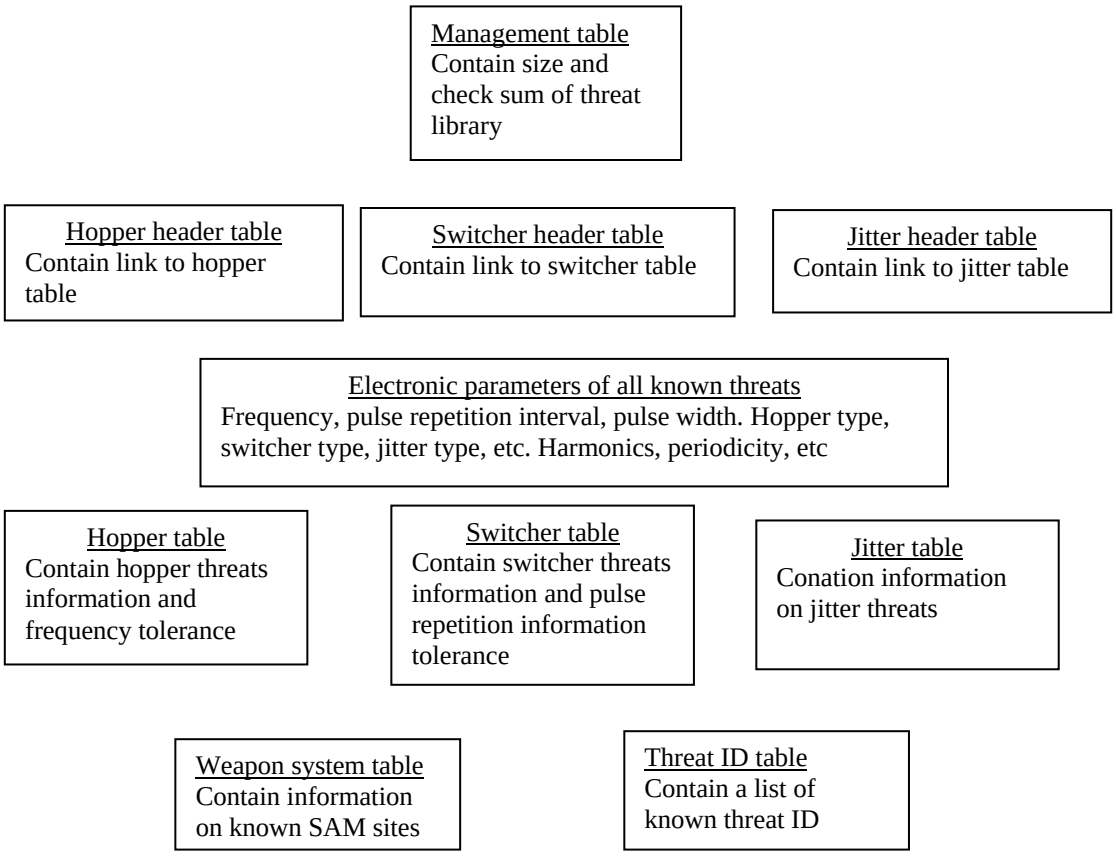


Figure 41. A hypothetical threat library.

**THIS PAGE INTENTIONALLY LEFT BLANK**

# IV. SPATIAL CORRELATION IN COMBAT ENVIRONMENT

The main objective of this chapter is to apply the spatial correlation concepts presented in Chapter III to some scenarios [1]. The scenarios to be addressed include; single emitter and single site correlation, single emitter and multiple sites correlation, multiple emitters and single site correlation. The operational advantages and loopholes of spatial correlation will be also addressed in this chapter.

It is important to state the rules for applying spatial correlation before proceeding to the next section. These rules can be summarized by the matrix show in Figure 42.

| **Ellipse size** | Big | Medium | Small |
|---|---|---|---|
| Big ( CEP > 10000m) | YES | YES | NO |
| Medium(CEP 5000m - 10000m) | YES | YES | YES |
| Small( CEP < 3000m) | NO | YES | YES |

Figure 42. The matrix for the spatial correlation decision of two ellipses representing likely emitter locations.

The correlation between a big and a small ellipse should be forbidden for the following reasons. First, a lot of uncertainty in the spatial location of the third ellipse will result if a big ellipse is to be combined with a small ellipse. Second, the improvement in CEP of the resultant ellipse will be insignificant. Third, the likelihood of making a false correlation is very high.

For the rest of this chapter, some scenarios will be addressed. The WSID of the active threats detected by the ELS are assumed to be the same as that of the preplanned SAM sites. Therefore, only the spatial locations of the threats will be considered for correlation. The possible decisions to be made are as follows:

1) Correlate an emitter to a preplanned site if the value of likelihood function exceed threshold (using equations 3.17 and 3.18).

2) Discorrelate an emitter from a preplanned site if the value of likelihood function falls below threshold.

3) Form a new site if the CEP of the uncertainty ellipse of the detected emitter reached 3000 meters and no correlation with preplanned sites can be established.

## A. SINGLE EMITTER VERSUS SINGLE SITE CORRELATION

In this scenario, an emitter was detected spatially close to a preplanned site. The emitter remains active throughout the flight and its probability of spatial correlation with the preplanned site exceeds the threshold value and hence established. See Figure 43.

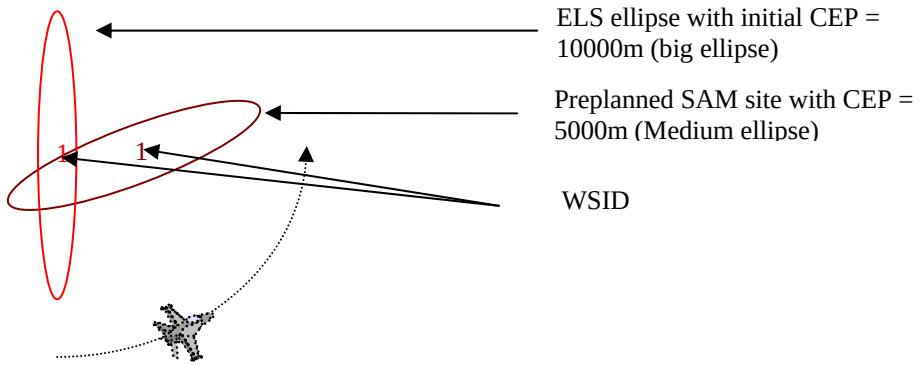


Figure 43. An example of a single emitter versus single site correlation.

The ELS ellipse is combined with the preplanned ellipse (using Equations 3.22 and 3.23) to form a resultant ellipse. There is a sudden drop in the CEP of the resultant ellipse, compared with the parent ellipses, when it is initially formed. It is this sudden drop in the CEP that made major contribution to the situation awareness of the combat environment. Thereafter, the CEP of the ELS and resultant ellipses improve only gradually. The CEP of the preplanned site remains constant throughout. See Figure 44.

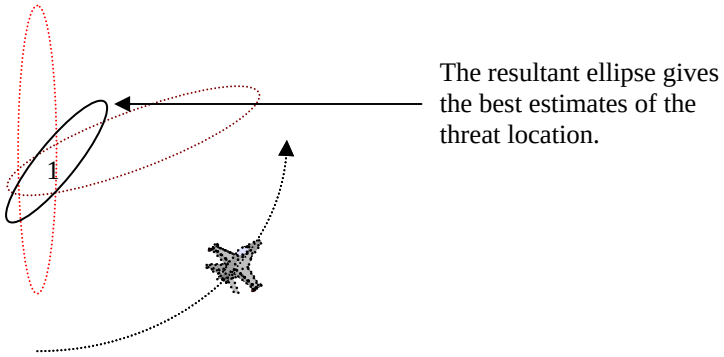


Figure 44. Combination of ELS and preplanned ellipse.

## B. SINGLE EMITTER VERSUS MULTIPLE SITES CORRELATION

In this scenario, an emitter was detected spatially close to two preplanned sites. The emitter remains active throughout the flight and the probabilities of spatial correlation with each of the preplanned sites exceed the threshold value. Spatial correlation is established with the preplanned site that has the higher probability value.

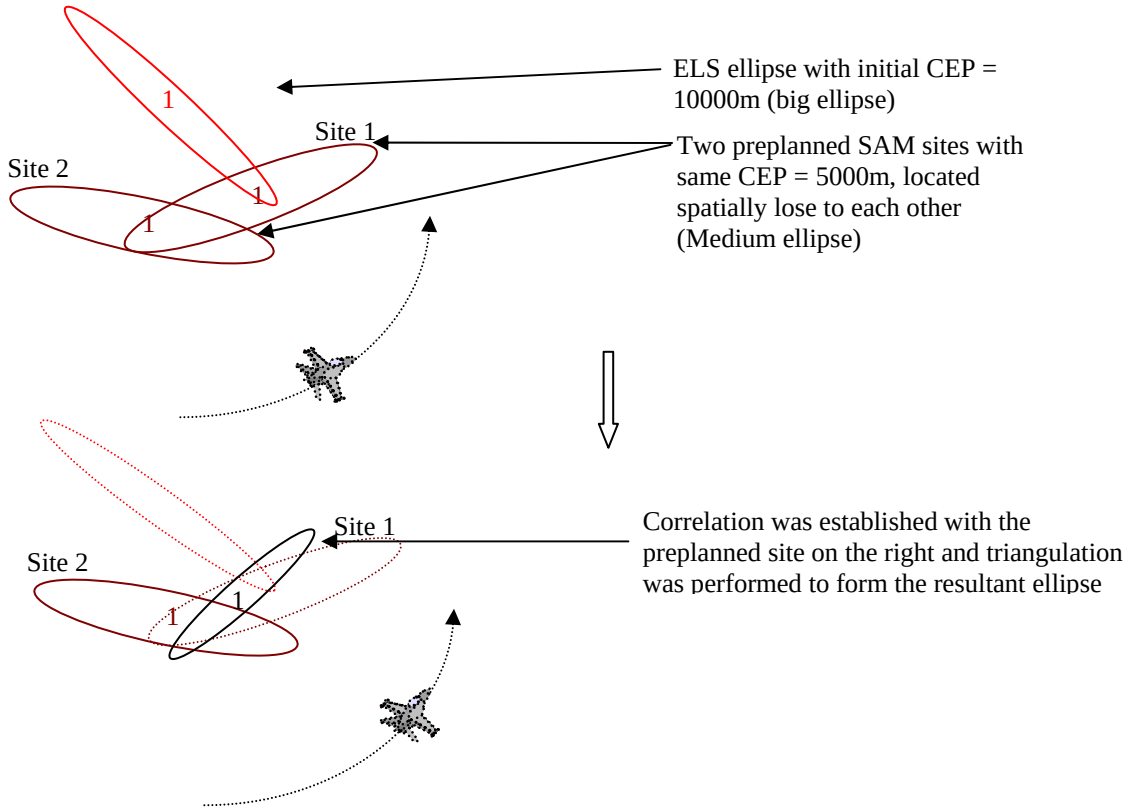


Figure 45. An example of single emitter versus multiple sites correlation.

The emitter is correlated with one of the site that has the higher probability value. After correlation has been established between the ELS threat and one of the preplanned sites, called this site 1, no further attempt will be made to correlate the correlated threat to any other available non-correlated preplanned sites (site 2).

When the CEP of the ELS ellipse improves, the threat location updates causes the correlation established initially to be discorrelated, i.e. the probability value falls below the threshold. The resultant ellipse is 'erased' and original parent ellipses are restored. In this case, the ELS ellipse is restored using the current available ELS data and the preplanned ellipse remain unchanged. See figure 46.

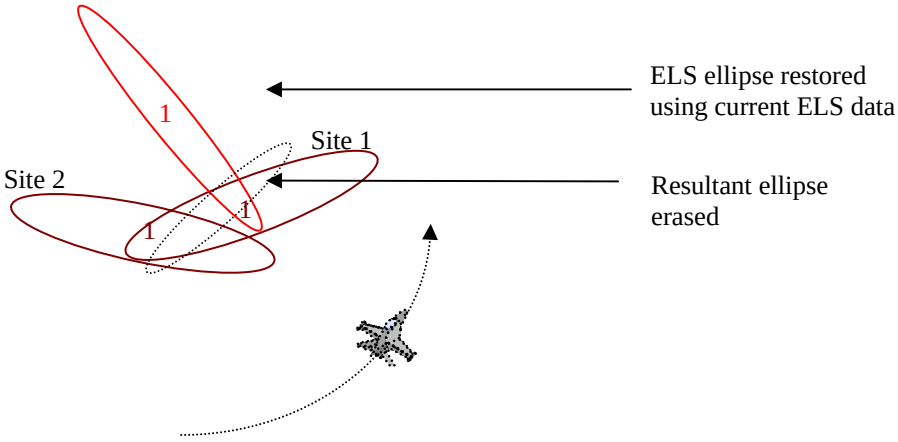


Figure 46. The combination of ELS and preplanned ellipse.

After discorrelation with site 1 is completed, the spatial correlation of the ELS threat with site 2 is attempted. If no correlation can be established, a new site is formed when the CEP of the ELS ellipse reaches 3000 meters.

## C. MULTIPLE EMITTERS VERSUS SINGLE SITE CORRELATION (SYSTEM WEAKNESS)

One of the generic problems in using a probabilistic approach to make a correlation decision will be addressed in this section. In this scenario, two emitters are active and only one of them (emitter 1) is supposed to correlate with the preplanned site. (Assume that this is a flight test scenario and the correct emitter to site correlation is known). See Figure 47. Since emitter 2 is also spatially close to the preplanned site, correlation is established.

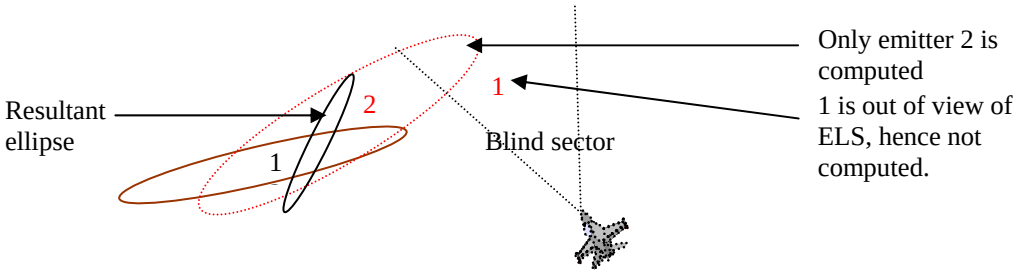


Figure 47. Emitter 1 and 2 are located spatially close to each other and emitter 1 is planned to correlate with the preplanned site. However, emitter 1 is in the blind zone of the ELS and hence not computed.

The aircraft changes its flight profile and ELS compute emitter 1. But correlation between emitter 1 and the preplanned site cannot be established. Emitter 1 forms a new site when the CEP of its uncertainty ellipse reaches 3000 meters. Emitter 2 discorrelates from the preplanned site. As a result, the new site formed by emitter 1 is overlaid on the preplanned site, instead of correlating with it.

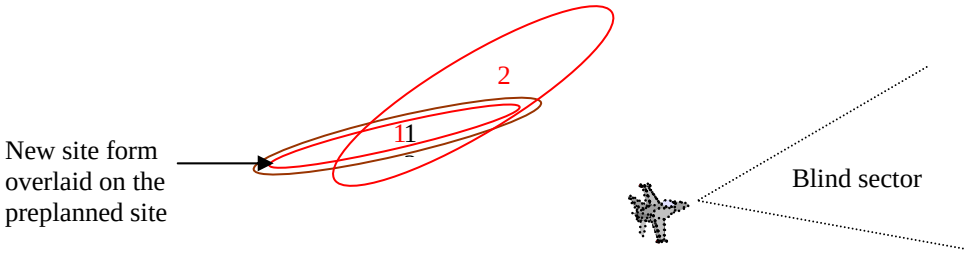


Figure 48. Formation of two sites instead of a correlated site.

Before ending this chapter, it is important to point out a realistic war time scenario, which was observed during Operation Desert Storm in 1991. This scenario also illustrates the importance of performing spatial correlation. A stationary ground emitter was switched on and off intermittently to avoid being intercepted by onboard sensors. If the ELS is to be operated alone, the CEP of the uncertainty ellipse will not achieve any significant improvement from its initial CEP. This is because the ELS will delete the emitter from its track when it is switched off. When the emitter is switched on again, the ELS will regard it as a new threat and start a new track for computation. With spatial correlation, the desired CEP may be achieved if correlation with the preplanned site is established.

**THIS PAGE INTENTIONALLY LEFT BLANK**

# V. SYSTEM ENHANCEMENTS

In this chapter, a potential weakness of the system and a recommended solution to the problem are addressed In Chapter IV, the strengths and weakness of spatial correlation were illustrated. The use of the extended Kalman filter algorithms and hence the formation of the resultant ellipse has significantly improved the time required to acquire the desired CEP of the uncertainty ellipse. The probabilistic approach and heuristic threshold value that were used to establish spatial correlation resulted in false correlation in some cases, especially in cases where there were multiple emitters. But in some cases, the system was able to identify and correct the mistake when the CEP of the sites improved.

The weakness of the system is manifested when the active emitter falls in the blind sector of the ELS, resulting in an unredeemable situation. This weakness in the system can be partially eliminated by flying a two aircraft sortie[6], in which each aircraft is installed with ELS and a data-link for data transfer purposes [1]. The flight profile for each of the aircraft should always cover the blind sector of its partner and vice versa. The data received by one of the aircraft is sent to the other for computation via data-link. In this way, the situational awareness of both aircraft is improved. Figure 49 shows how the use of two aircraft overcomes the weakness of the system.

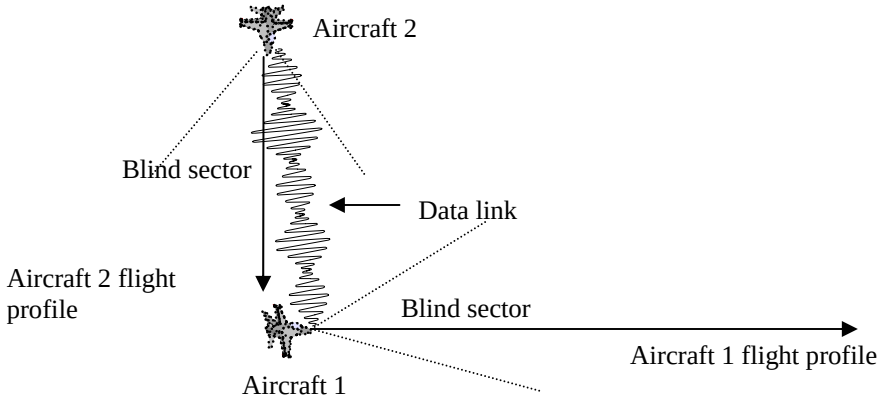


Figure 49. A two aircraft flight profile that improves the coverage of the ELS.

[6] Launching a two aircraft sortie is one of the solutions. Another alternative is to install a few ELS onboard such that each ELS cover the blind sector of the others.

When two onboard ELS are available, electronic correlation can be exploited [1]. To establish electronic correlation, the fundamental electronic parameters such as frequency, pulse repetition interval and pulse width have to be matched to within a certain tolerance[7], defined in the threat library. Spatial correlation is performed when electronic correlation is established in order to establish that the active emitter detected by the two sensors is the same. See Figure 50.

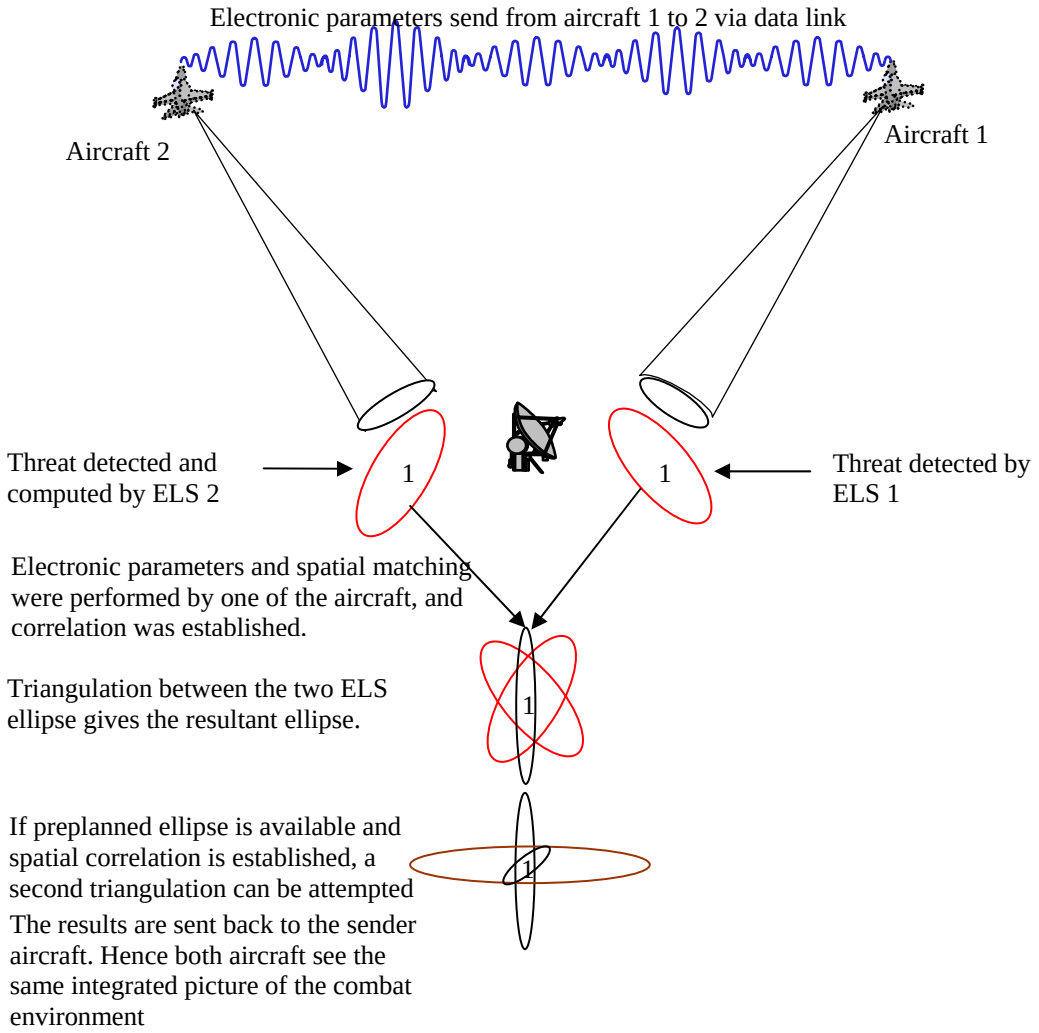


Figure 50. The electronic and spatial correlation in a two ELS scenario.

[7] The tolerance has to be defined in order to perform an electronic parameters match. Because of atmospheric attenuation, a measurement of electromagnetic pulses made in different spatial locations by the same sensor produces different results.

# VI. CONCLUSION

A real time method of constructing an optimal route for aircraft sortie to avoid kill envelopes in a combat environment has been developed. This technique improves upon the conventional approaches such as the Dijkstra's and Bellman Ford algorithms. The optimal route increases the safety of the aircraft by reducing the aircraft flight time and risk when flying to its destination.

In addition, a technique was developed to establish spatial correlation and to combine the uncertainty ellipses through the use of Extended Kalman Filter algorithms to increase the situational awareness of the operators. Hence, the operator is provided with the most updated locations of the enemies' SAM sites. The above is summarized in Figure 51.

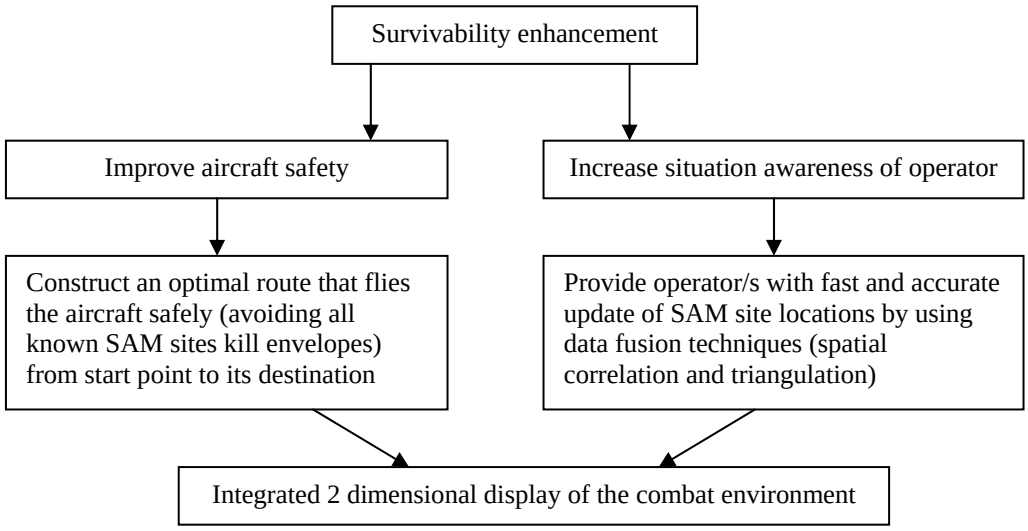


Figure 51. A summary of the survivability enhancement techniques addressed in this thesis.

On the average, the time required to construct an optimal route is about 200ms. The error of the computed route does not exceed 8% compared with those computed manually on a case by case basis. However, the technique used to construct the optimal route does not work if the SAM sites are not stationary.

With the combat environment dominated by more sophisticated and robust weapon systems such as the laser (LS) guided missiles and infrared (IR) seeking missiles, there is an urgent requirement for the development of an automated, effective and reliable self-protection system to enhance the survivability of aircraft. Further recommended work includes incorporating laser warning systems (LWS) and missile warning systems (MWS) with the ELS to form an integrated system that can provide early warning and localization of potential RF, LS and IR threats.

# APPENDIX

Derivation of equation (3.22) and (3.23):

$\hat{\mathbf{m}} = \mathbf{x} + K[\hat{\mathbf{m}}_2 - \mathbf{h}\hat{\mathbf{m}}_1]$, where **h** is unity. Using equation 3.9 and 3.10

$K = \mathbf{PH}^T(\mathbf{HPH}^T + \mathbf{R})^{-1} = \mathbf{P}(\mathbf{P} + \mathbf{R})^{-1}$, where **H** = **I** (identity matrix)

Therefore,

$$\hat{\mathbf{m}} = \hat{\mathbf{m}}_1 + \mathbf{P}(\mathbf{P}+\mathbf{R})^{-1}[\hat{\mathbf{m}}_2 - \hat{\mathbf{m}}_1]$$
$$= [\mathbf{I} - \mathbf{P}(\mathbf{P}+\mathbf{R})^{-1}]\hat{\mathbf{m}}_1 + \mathbf{P}(\mathbf{P}+\mathbf{R})^{-1}\hat{\mathbf{m}}_2$$
$$= [(\mathbf{P}+\mathbf{R})(\mathbf{P}+\mathbf{R})^{-1} - \mathbf{P}(\mathbf{P}+\mathbf{R})^{-1}]\hat{\mathbf{m}}_1 + \mathbf{P}(\mathbf{P}+\mathbf{R})^{-1}\hat{\mathbf{m}}_2$$
$$= \mathbf{R}(\mathbf{P}+\mathbf{R})^{-1}\hat{\mathbf{m}}_1 + \mathbf{P}(\mathbf{P}+\mathbf{R})^{-1}\hat{\mathbf{m}}_2$$

$\mathbf{z} = \mathbf{Ax} + \mathbf{By}$,

where **A** and **B** are constant matrices. The combine covariance matrix of the ellipses can be represented by

$$\mathrm{COV} = \begin{bmatrix} \mathbf{R} & \mathbf{0} \\ \mathbf{0} & \mathbf{P} \end{bmatrix}$$

The cross term vanishes because the sensor inputs are independent of the preplanned data. Therefore, the covariance of the resultant ellipse, **Q** is:

$$\mathbf{Q} = \begin{bmatrix} \mathbf{R}(\mathbf{P}+\mathbf{R})^{-1} & \mathbf{P}(\mathbf{P}+\mathbf{R})^{-1} \end{bmatrix} \begin{bmatrix} \mathbf{R} & \mathbf{0} \\ \mathbf{0} & \mathbf{P} \end{bmatrix}$$
$$= \mathbf{R}(\mathbf{P}+\mathbf{R})^{-1}\mathbf{P}\,(\mathbf{P}+\mathbf{R})^{-1}\mathbf{R} + \mathbf{P}(\mathbf{P}+\mathbf{R})^{-1}\mathbf{R}\,(\mathbf{P}+\mathbf{R})^{-1}\mathbf{P}$$

where

$\mathbf{A} = \mathbf{R}(\mathbf{P}+\mathbf{R})^{-1}$, $\mathbf{B} = \mathbf{P}(\mathbf{P}+\mathbf{R})^{-1}$, $\mathbf{A}^T = (\mathbf{P}+\mathbf{R})^{-1}\mathbf{R}$ and $\mathbf{B}^T = (\mathbf{P}+\mathbf{R})^{-1}\mathbf{P}$

Let

$\mathbf{\Pi} = \mathbf{R}\,(\mathbf{P}+\mathbf{R})^{-1}\mathbf{P}$

Since $\mathbf{\Pi}$ represents the covariance matrix of the ellipse, whose cross terms are zeros,

$$\mathbf{\Pi}^T = \mathbf{\Pi}$$

Therefore,

$$\begin{aligned}
\mathbf{Q} &= \mathbf{\Pi}\,(\mathbf{P}+\mathbf{R})^{-1}\mathbf{R} + \mathbf{\Pi}^T\,(\mathbf{P}+\mathbf{R})^{-1}\mathbf{P} \\
&= \mathbf{\Pi}\,[\,(\mathbf{P}+\mathbf{R})^{-1}\mathbf{R} + (\mathbf{P}+\mathbf{R})^{-1}\mathbf{P}\,] \\
&= \mathbf{\Pi}(\mathbf{P}+\mathbf{R})^{-1}(\mathbf{P}+\mathbf{R}) \\
&= \mathbf{\Pi} \\
&= \mathbf{R}(\mathbf{P}+\mathbf{R})^{-1}\mathbf{P}
\end{aligned}$$

# LIST OF REFERENCES


[1] Proprietary of Singapore Technologies Aerospace. Republic of Singapore. 1998.

[2] Professor Robert G. Hutchins “Optimal Estimation, Kalman Filters And Target Tracking”. Naval Postgraduate School. 31th March 1997.

[3] Filippo Neri. “Introduction To Electronic Defense Systems”. 2nd Edition.

[4] B.T Jaynes. “Probability Theory: the Logic Of Science”. Professor of Physics Washington University St. Louis, MO 63130 U.S.A.

[5] Ömer Benli. “Dynamic Programming”. Bilkent University. 1999.[ http://benli.bcc.bilkent.edu.tr/~omer/research/dynprog.html].

[6] Don J.Torrieri. “Statistical Theory of Passive Location Systems”. U.S .Army Countermeasures / Counter-Countermeasures Center.

**THIS PAGE INTENTIONALLY LEFT BLANK**

# INITIAL DISTRIBUTION LIST

1. Defense Technical Information Center
   Ft. Belvoir, Virginia

2. Dudley Knox Library
   Naval Postgraduate School
   Monterey, California

3. Professor Daphne Kapolka
   Department of Physics
   Naval Postgraduate School
   Monterey, California

4. Professor Robert Hutchins
   Department of Electrical and Computer Engineering
   Naval Postgraduate School
   Monterey, California

5. Professor Yeo Tat Soon
   Temasek Defence Systems Institute
   National University of Singapore
   Republic Of Singapore

6. Mr. Seow Yoke Wei
   Singapore Ministry of Defense